Stationary complementary energy high-order theory for the static analysis of beams

Phe Van Pham[a,1], Magdi Mohareb[a], and Amir Fam[b],

[a] Department of Civil Engineering, University of Ottawa, Ottawa, ON, Canada K1N 6N5

[b] Department of Civil Engineering, Queen's University, Kingston, ON, Canada K7L 3N6

Abstract

A high-order theory is developed for the analysis of beams with general mono-symmetric cross-sections. The theory represents the nonlinear distribution of the longitudinal normal stress across the section depth by a polynomial series expansion up to any order as specified by the analyst. The corresponding shear and transverse normal stresses are obtained by satisfying the 2D infinitesimal stress-flow equilibrium conditions. The resulting statically admissible stress fields are then used in conjunction with the principle of stationary complementary strain energy to formulate the governing compatibility equations and boundary conditions. Closed form solutions are then developed for general loading and boundary conditions. Comparisons with the theory of elasticity and 3D finite element analysis predictions showcase the ability of the present theory to naturally capture shear deformation effects, transverse normal stress effects, nonlinear longitudinal normal stress distributions in deep beams, as well as the effect of support height. Unlike conventional beam solutions that are based on postulated kinematic assumptions, which tend to converge to the displacement response from below, the present theory avoids introducing any kinematic assumptions and is shown to converge to the solution from above. The theory is applicable to beams with doubly symmetric or mono-symmetric cross-sections, with isotropic or orthotropic materials, and subjected to general loading and boundary conditions. The theory is shown to offer advantages compared to other theories when modelling deep beams and/or beams with supports that are offset from the centroidal axis.

Keywords: High order beam theory, principle of stationary complementary energy, shear deformation, deep beams, and orthotropic material.

This article is to be cited as
Pham PV, Mohareb M and Fam A (2020), Stationary complementary energy high-order theory for the static analysis of beams, Annals of Solid and Structural Mechanics, 12, 199–220

The copy-edited version of this article is available at https://doi.org/10.1007/s12356-019-00054-3

[1] Corresponding author. Tel: (+1) 613 562 5800 ext. 6066;

Email: ppham040@uottawa.ca (P. V. Pham)

List of Symbols

The following notation has been used in the paper

$\{\mathbf{a_i}\}_{m\times 1}$	Vectors of displacement multipliers defined in Equation (17).
$A_{0\sigma}, A_{0\tau}$	parts of the cross-section $z_e = 0$ where the longitudinal stresses and shear stresses are respectively prescribed.
$A_{L\sigma}, A_{L\tau}$	parts of the cross-section $z_e = L$ where the longitudinal stresses and shear stresses are respectively prescribed.
A_{0w}, A_{0v}	parts of the cross-section $z_e = 0$ where the longitudinal and transverse stresses are respectively prescribed.
A_{Lw}, A_{Lv}	parts of the cross-section $z_e = L$ where the longitudinal and transverse stresses are respectively prescribed.
$\{\mathbf{A}\}$	Vector of integration constants arising from integrating the compatibility equations (defined in Equation 27)
$\left[\mathbf{b_{ij}}\right]$, ($i = 1,...,7$, $j = 1,2,...,4$)	Matrices depending solely on the mechanical properties and beam cross-section, introduced in Equations. (39-45) and defined in Appendix 2
$b(y)$	width of the beam cross-section as a function of the y-coordinate
c_i	Eigen value i of the quartic eigen-value problem defined in Section 4.3: $\left\|\left[c_i^4\mathbf{C_{22}} - \left(\hat{\mathbf{I}}_1\mathbf{C_{12}} + \mathbf{C_{12}^T}\hat{\mathbf{I}}_1^{\mathbf{T}} + \tilde{\mathbf{I}}_1\mathbf{C_{33}}\tilde{\mathbf{I}}_1^{\mathbf{T}}\right)c_i^2 + \hat{\mathbf{I}}_1\mathbf{C_{11}}\hat{\mathbf{I}}_1^{\mathbf{T}}\right]\right\| = 0$
$\mathbf{C_{11}}$, $\mathbf{C_{12}}$, $\mathbf{C_{22}}$, $\mathbf{C_{33}}$	compliance matrices defined in Equation (8)
$\mathbf{d_1}(z)$, $\mathbf{d_2}(z)$, $\mathbf{d_3}(z)$	traction-dependent displacement vectors defined in Equation (9a-c)
$\left[\mathbf{e}(z)\right]_{4m\times 4m}$	Matrix of exponential functions based on eigenvalues c_i (defined in Eq. 27)
E_y, E_z ,	longitudinal and transverse moduli of elasticity, respectively
$\{\mathbf{f}\}_{m\times 4m}$	Matrix of eigenvectors (defined in Equation 27)
$\mathbf{F}(z)$ $\hat{\mathbf{F}}(z)$ $\tilde{\mathbf{F}}(z)$	Vectors of unknown stress functions $F_i(z)$ introduced in Equation 3a-c.
$F_i(z)$	A-priori unknown stress functions $i = 1,2...,n$ appearing in the definition of the longitudinal normal stress field in Eq. (1).
$\{\mathbf{F_H}(z)\}$	Homogeneous solution of the compatibly equations, provided in Equation 26
$\{\mathbf{F_{P1}}(z)\}$	Particular solution of the compatibility equations corresponding to vector $\mathbf{R_{p1}}(z)$, provided in Equation 28.
$\{\mathbf{F_{P2}}(\mathbf{z})\}$	Particular solution of the compatibility equations corresponding to vector $\mathbf{R_{p2}}(z)$, provided in Equation 32
G	Shear modulus
$\hat{\mathbf{I}}_1 - \hat{\mathbf{I}}_5$, $\tilde{\mathbf{I}}_1 - \tilde{\mathbf{I}}_3$	Matrices defined in terms of the identity matrix $\mathbf{I}$ introduced in Equation 12 and used to extract the relevant terms from compliance, displacement, and stress function vectors/matrices in Equation 11
$\{\mathbf{L}_i\}_{m\times 1}$	Load vectors introduced in Eqs. (39-45), and defined in Appendix 2

h_1, h_2	distances from the origin to the top and bottom fibres, respectively (Fig.1)
m	Number of compatibility equations $m = n - 2$ and defining the size of vector $\mathbf{F}(z)_{m\times 1}$ introduced in Equation (2a-c)
n	Number of functions $F_i(z)$ used to define the longitudinal stress field in Equation (1).
$M(z_i)$	bending moment at coordinate z_i as defined in Equation (4)
$N(z_i)$	Normal force at coordinate z_i as defined in Equation (4)
$p_y(y,z)$, $p_z(y,z)$	transverse and longitudinal body forces, respectively (Figure 1)
$Q(z_i)$,	Shearing force at coordinate z_i as defined in Equation (4)
$\mathbf{R_{p1}}(z), \mathbf{R_{p2}}(z)$	Deformation vector functions appearing at the right hand sides of compatibility equations (Equations 18)
U^*	complementary internal strain energy
V^*	load potential energy
$\overline{V}(z_e)$	Specified transverse displacement at $(z_e = 0, L)$ (defined in Figure 2).
$\overline{W}(z_e)$	Specified longitudinal displacement at $(z_e = 0, L)$ (defined in Figure 2).
$\alpha_i(y), \beta_i(y)$	functions of the *y*- coordinate appearing in Eqs. 5b-c, 55-59 and defined in Eq. 53
$\overline{\alpha}_i, \hat{\alpha}_i$	Constants defined in Eq. 55 appearing in the definitions of constants $\varsigma_{11}, \varsigma_{12}, \varsigma_{21}, \varsigma_{22}, \varsigma_{31}, \varsigma_{32}, \varsigma_{41}, \varsigma_{42}$, and $\varsigma_{13i}, \varsigma_{23i}, \varsigma_{33i}, \varsigma_{43i}$ as defined in Eq. 56.
ς_{11} , ς_{21}	Constants appearing in the definition of $\sigma_z^*(y,z), \sigma_y^*(y,z)$ that depend on the applied loads, defined in Equation (56)
$\eta_{12}(y), \eta_{13}(y), \eta_{14}(y), \eta_{22}(y)$	Distribution functions of the *y*- coordinate defined in Eq. (59) used to define vectors $\hat{\boldsymbol{\chi}}(y)$ and $\tilde{\boldsymbol{\chi}}(y)$
$\overline{\theta}(z_e)$	specified rotation at beam-ends $(z_e = 0, L)$ a defined in Fig. 2
$\lambda_{1i}, \lambda_{2i}$	functions defined in Equation 58 appearing in the definitions of $\xi_{1i}(y), \xi_{2i}(y), \xi_{3i}(y)$
μ_{yz}, μ_{zy}	Poisson's ratios
$\boldsymbol{\xi_1}(y), \boldsymbol{\xi_2}(y), \boldsymbol{\xi_3}(y)$	Vectors of functions of *y* that depend upon the cross-section geometry and applied tractions as defined in Equation (61).
$\xi_{ij}(y)$	Distribution functions of the *y*- coordinate defined in Equation (59) used to define the vectors $\boldsymbol{\xi_1}(y), \boldsymbol{\xi_2}(y), \boldsymbol{\xi_3}(y)$
π^*	total complementary energy
$\rho_1(z)$, $\rho_2(z)$	Functions appearing in the definition of $\sigma_z^*(y,z), \sigma_y^*(y,z), \tau^*(y,z)$ that depend on the applied loads, defined in Equation (58)
σ_z, σ_y, τ	Longitudinal, transverse, and shear stress fields
$\sigma_z^*(y,z), \sigma_y^*(y,z), \tau^*(y,z)$	Load dependent terms defined in Equations (5a-c)
$\tau(y,z)$	transverse shear stress
$\{\phi_i\}^T = \langle 1 \quad \phi_{2,i} \quad \cdots \quad \phi_{m,i} \rangle$	Eigen vector i of the quartic eigen-value problem defined in Section 4.3; $\left\| \left[c_i^4 \mathbf{C_{22}} - \left(\hat{\mathbf{I}}_\mathbf{1} \mathbf{C_{12}} + \mathbf{C_{12}^T} \hat{\mathbf{I}}_\mathbf{1}^\mathbf{T} + \tilde{\mathbf{I}}_\mathbf{1} \mathbf{C_{33}} \tilde{\mathbf{I}}_\mathbf{1}^\mathbf{T} \right) c_i^2 + \hat{\mathbf{I}}_\mathbf{1} \mathbf{C_{11}} \hat{\mathbf{I}}_\mathbf{1}^\mathbf{T} \right] \right\| = 0$
$\hat{\boldsymbol{\chi}}(y)$, $\tilde{\boldsymbol{\chi}}(y)$,	functions of *y* that depend upon the cross-section geometry and applied tractions and are defined in Equation (61)

$\psi_{ij}(y)$	functions of the *y*- coordinate, as defined in Equation (59)
$\boldsymbol{\psi}_1(y), \boldsymbol{\psi}_2(y), \boldsymbol{\psi}_3(y)$	Vectors of functions $\psi_{ij}(y)$ that appear in the definition of $\hat{\boldsymbol{\chi}}(y)$ and $\tilde{\boldsymbol{\chi}}(y)$

1. Introduction and Literature Review

The conventional Euler Bernoulli beam is based on the assumption that plane sections remain plane after deformation and normal to the beam axis. The normality condition implies the omission of shear deformation. Thus, the theory is able to reliably predict the response of long-span beams where shear deformations are negligible, but underestimates deflections for short-span beams where shear deformation are known to be influential. The Timoshenko beam theory, where the plane section assumption is retained but the normality to the beam axis is relaxed, is an improvement over the Euler-Bernoulli beam theory in that it accounts for shear deformation effects. However, the plane section assumption creates a non-zero shear strain, and hence a non-zero shear stress, at the outermost fibers, which violates the traction boundary conditions as the externally applied shear traction typically vanishes at the outermost fibers of the beam. As a result, the Timoshenko theory tends to overestimate the stiffness of the beam (Mucichescu 1984). Other variations of the Timoshenko beam theory involve shear modification factors that depend on the cross-section shape (e. g., Timoshenko 1921, Cowper 1966, Stephen 1980) and the type of analysis, whether static or dynamic, (Mindlin 1953, Heyliger and Reddy 1988). Another limitation of the Timoshenko beam theory is the fact that it omits the normal stresses in the transverse direction. As a result, while it satisfies the vertical equilibrium condition for the whole cross-section in a global integral sense, it violates the vertical equilibrium requirement in an infinitesimal sense. Also, both the Euler Bernoulli and Timoshenko beam theories predict linear stress profiles, which are appropriate approximations for long-span beams but are inconsistent with elasticity solutions for deep beams (e.g., Timoshenko and Goodier 1970) and advanced beam theories (e.g., Carrera and Guinta 2010). Also, conventional beam theories adopt the centroidal axis as a reference. By default, such solutions locate transverse restraints at the section centroid. As such, the modelling of supports that are offset from the centroid requires special considerations (e.g.,Wight and Parra (2002), Erkmen and Mohareb (2006a,b), Wu and Mohareb (2011)).

To remedy the limitations of the conventional beam theories, higher order theories for beams with rectangular cross-sections were developed based on the principle of stationary potential strain energy. This includes the work of Stephen and Levinson (1979), Levinson (1981), Reddy (1984), Heyliger and Reddy (1988), Shu and Sun (1994), and Jha et al (2013), all assumed a cubic distribution of the longitudinal displacement along the height. Further advancements were proposed in the work of Carrera and Guinta (2010), Carrera et al (2015), and Groh and Weaver (2015) where the longitudinal displacement field was assumed to follow higher order polynomials.

Numerous researchers developed and investigated high order beam theories. A non-exhaustive review includes the work of Bhimaraddi and Chandrashekhara (1993) who conducted a comparative study on high order beam theories with sinusoidal, cubic, quartic, quintic, and sixth-order polynomial displacement profiles, and Karama et al. (2003) who developed a shear deformation beam theory based on an exponential displacement profile. Ding et al. (2005) developed an analytical solution for fixed beams under uniform load based the Airy stress function approach. Reddy (2007) reformulated the Euler-Bernoulli, Timoshenko, Reddy, and Levinson theories using nonlocal differential constitutive relations. Mechab et al. (2008) conducted a comparative study on high-order flexural theories as applied to deep beams. Challamel (2011) adopted a variationally consistent approach to conduct a comparative study of shear deformable beam theories. Guangyu and Voyiadjis (2011) developed a sixth-order theory for shear deformable beams. Sun et al. (2015) investigated the effect of boundary conditions on the Reddy higher-order shear beam theory. Geng et al. (2017) formulated a variationally consistent high-order beam theory. Nolde et al. (2018) developed an asymptotic

higher-order theory for a beam with the rectangular cross section. Core et al. (2018) used the asymptotic expansion method to formulate higher order beam models.

The majority of the above solutions omit transverse stresses, are restricted to rectangular cross-sections, and/or consider supports located at the centroid. In this respect, the present study aims at overcoming these limitations by developing a family of solutions that capture transverse stresses, model beams with general monosymmetric cross-sections with the capability of seamlessly modelling supports that are offset from the centroid. Also, a common theme in the above high-order theories is that they postulate kinematic assumptions satisfying compatibility in an exact point-wise sense, and then use the principle of stationary potential energy to formulate approximate equilibrium equations. The approach contrasts with that based on the principle of stationary complementary strain energy, adopted in the present study, whereby stress fields that exactly satisfy the infinitesimal stress equilibrium conditions are postulated and then used within the stationary complementary energy principle to formulate approximate compatibility equations. Examples of such developments include the work of Chen and Cheng (1983) on adhesive bonded shear laps, Erkmen and Mohareb (2006c) on torsional analysis of thin-walled members, Erkmen and Mohareb (2008a,b) on the lateral torsional buckling of beams, Zhao et al. (2014) for lap joints, and most recently Pham et al. (2018) on the analysis of multilayered beams. Within the above context, the present study aims at formulating the governing field equations and boundary conditions, for a high-order beam theory based on the principle of stationary complementary strain energy. The treatment avoids adopting kinematic assumptions made in conventional and high order beams. Instead, it is based on a polynomial series expansion of the longitudinal normal stress field as a function of the transverse coordinate across the depth of the section, up to a polynomial order specified by the analyst. A general solution technique is then developed to provide a closed form solution for the resulting coupled compatibility equations. Unlike the study in Pham et al. (2018) which developed a complementary energy based finite element formulation, the present study explicitly formulates the compatibility equations and boundary conditions of the problem.

2. Statement of the Problem

A prismatic beam of span L and an arbitrary mono-symmetric cross-sectional area A, made of an orthotropic material, is loaded by transverse and longitudinal body forces $p_y\left(y,z\right)$ and $p_z\left(y,z\right)$ and surface tractions $\sigma_y\left(h_1,z\right),\tau\left(h_1,z\right),\sigma_y\left(h_2,z\right),\tau\left(h_2,z\right)$ (Figure 1.a-b). Ends $z_e=0,L$ are assumed are subjected to specified longitudinal traction $\sigma_z\left(z_e,y\right)$ and transverse shear traction $\tau\left(z_e,y\right)$ on the parts of the cross-section $A_{0\sigma},A_{0\tau}$ at $z_e=0$, and $A_{L\sigma},A_{L\tau}$ at $z_e=L$ while longitudinal displacement $w\left(z_e,y\right)$ and transverse displacement $v\left(z_e,y\right)$ are specified on the remaining parts of the cross-section (i.e., A_{0w},A_{0v}, A_{Lw},A_{Lv}). It is required to develop a high-order beam theory that captures the effect of normal longitudinal stresses σ_z , normal transverse stresses σ_y , and shearing stresses τ (Figure 1.c). The theory is intended to capture the nonlinear stress distribution along the beam height, as may be the case, for example, in deep beams. The solution sought is based on the principle of stationary complementary energy.

Figure 1 Beam tractions and body forces

3. Overview of past solution for statically admissible stress fields

The longitudinal normal stresses field is assumed to take the form

$$\sigma_z\left(y,z\right)=\sum_{i=1}^{n}y^{i-1}F_i\left(z\right) \tag{1}$$

where $F_i(z)$ are unknown functions of longitudinal coordinate z, y is the transverse coordinate and n is a positive integer. For the stress field postulated in Eq. (1) to be statically admissible, it needs to satisfy two shear-flow equilibrium conditions (Figure 1c):

$$\begin{aligned}\frac{\partial}{\partial y}\left[b(y)\sigma_y(y,z)\right]+\frac{\partial}{\partial z}\left[b(y)\tau(y,z)\right]&=b(y)\,p_y(y,z)\\ \frac{\partial}{\partial y}\left[b(y)\tau(y,z)\right]+\frac{\partial}{\partial z}\left[b(y)\sigma_z(y,z)\right]&=b(y)\,p_z(y,z)\end{aligned} \tag{2a-b}$$

From Eq. (1), by substituting into Eq. (2b), and integrating from $-h_1$ to y, one recovers the expression of shear stresses $\tau(y,z)$. Also, starting with the expression for $\tau(y,z)$, by substituting into Eq. (2a) and integrating from $-h_1$ to y, the transversal normal stresses $\sigma_y(y,z)$ is obtained. Then, by equating the stress fields $\tau(y,z)$ and $\sigma_y(y,z)$ to $\tau(h_2,z)$ and $\sigma_y(h_2,z)$ at the bottom face $y=h_2$, to satisfy the traction boundary conditions, functions $F_{n-1}(z)$ and $F_n(z)$ are related to the remaining functions $F_i(z)$ where $i=1,\ldots,n-2$. Finally, functions $F_{n-1}(z)$ and $F_n(z)$ are eliminated in the expression of the three stress fields. A similar procedure has been employed in (Pham et al. 2018) for multilayer beams. The statically admissible stress expressions sought for the present homogeneous beam can be recovered by setting to 1 the number of layers ($p=1$) in the expression in (Pham et al. 2018) to yield the following expressions:

$$\begin{aligned}\sigma_z(y,z) &= \hat{\boldsymbol{\chi}}(y)\hat{\mathbf{F}}(z) &&+\sigma_z^*(y,z)\\ \tau(y,z) &= \tilde{\boldsymbol{\chi}}(y)\tilde{\mathbf{F}}(z) &&+\tau^*(y,z)\\ \sigma_y(y,z) &= \boldsymbol{\xi}_3(y)\mathbf{F}''(z) &&+\sigma_y^*(y,z)\end{aligned} \tag{3a-c}$$

in which the unknown vectors $\mathbf{F}(z),\hat{\mathbf{F}}(z),\tilde{\mathbf{F}}(z)$ are defined as

$$\begin{aligned}\mathbf{F}(z)^{\mathbf{T}}_{1\times m} &= \left\langle F_1(z) \quad F_2(z) \quad \ldots \quad F_m(z)\right\rangle,\ m=n-2\\ \hat{\mathbf{F}}(z)^{\mathbf{T}}_{1\times 3(m+1)} &= \left\langle \mathbf{F}(z)^{\mathbf{T}}_{1\times m} \,\vdots\, \mathbf{F}(0)^{\mathbf{T}}_{1\times m} \quad z\mathbf{F}'(0)^{\mathbf{T}}_{1\times m} \,\vdots\, N(0) \quad zQ(0) \quad M(0)\right\rangle\\ \tilde{\mathbf{F}}(z)^{\mathbf{T}}_{1\times(2m+1)} &= \left\langle \mathbf{F}'(z)^{\mathbf{T}}_{1\times m} \,\vdots\, \mathbf{F}'(0)^{\mathbf{T}}_{1\times m} \,\vdots\, Q(0)\right\rangle\end{aligned} \tag{126}$$

and stress resultants at z_i (Figure 2.a) are defined as

$$N(z_i)=\int_{A_{iw}}\sigma_z(y,z_i)\,dA;\quad Q(z_i)=\int_{A_{i\tau}}\tau(y,z_i)\,dA;\quad M(z_i)=\int_{A_{iw}}y\sigma_z(y,z_i)\,dA \tag{4}$$

In Eqs. (3a-c), vectors $\hat{\boldsymbol{\chi}}(y)$, $\tilde{\boldsymbol{\chi}}(y)$, $\boldsymbol{\xi}_3(y)$ are known functions of *y* that depend upon the cross-section geometry and applied tractions and are defined in Appendix 1. Also, in (3a-c), the load dependent terms are

$$\begin{aligned}\sigma_z^*(y,z)&=\int_0^z\int_0^z\left[y^{n-2}\rho_1(z)+y^{n-1}\rho_2(z)\right]dz\,dz+z\left(y^{n-2}\varsigma_{11}+y^{n-1}\varsigma_{21}\right);\\ \tau^*(y,z)&=\bar{\tau}(y,z)-\int_0^z\left[\alpha_{n-1}(y)\rho_1(z)+\alpha_n(y)\rho_2(z)\right]dz-\alpha_{n-1}(y)\varsigma_{11}-\alpha_n(y)\varsigma_{21};\\ \sigma_y^*(y,z)&=\bar{\sigma}_y(y,z)+\beta_{n-1}(y)\rho_1(z)+\beta_n(y)\rho_2(z);\end{aligned} \tag{131 5a-c}$$

in which $\rho_1(z)$, $\rho_2(z)$, and ς_{11} and ς_{21} depend on the applied loads, and $\alpha_{n-1}(y)$, $\beta_{n-1}(y)$ $\beta_{n-1}(y)$, and $\beta_n(y)$ are functions of the transverse coordinate and are defined in Appendix 1.

4. Formulating the governing equations and closed form solution

4.1. Total complementary energy functional

The total complementary energy $\pi^* = U^* + V^*$ is the sum of the complementary internal strain energy U^* and the load potential energy V^* gained by the end forces. For an orthotropic material, the complementary strain energy is contributed by three stress fields σ_z, σ_y, τ (Pham 2018) is

$$U^* = (1/2)\int_L\int_A \left(\sigma_z^2/E_z + \sigma_y^2/E_y - 2\mu_{zy}\sigma_z\sigma_y/E_z + \tau^2/G\right)dAdz \tag{6}$$

where E_z, E_y are the longitudinal and transverse elasticity moduli, G is the shear modulus, and μ_{zy} and μ_{yz} are Poisson's ratios which satisfy the condition $\mu_{yz}/E_y = \mu_{zy}/E_z$. From Eqs. (3), by substituting into Eq. (6), one obtains

$$U^* = \int_L \frac{1}{2}\left\langle \hat{\mathbf{F}}(z) \quad \mathbf{F}''(z) \quad \tilde{\mathbf{F}}(z)\right\rangle^{\mathbf{T}} \begin{bmatrix} \mathbf{C_{11}} & \mathbf{-C_{12}} & \mathbf{0} \\ \mathbf{-C_{12}^T} & \mathbf{C_{22}} & \mathbf{0} \\ \mathbf{0} & \mathbf{0} & \mathbf{C_{33}} \end{bmatrix} \begin{Bmatrix} \hat{\mathbf{F}}(z) \\ \mathbf{F}''(z) \\ \tilde{\mathbf{F}}(z) \end{Bmatrix} + \left\langle \hat{\mathbf{F}}(z) \quad \mathbf{F}''(z) \quad \tilde{\mathbf{F}}(z)\right\rangle^{\mathbf{T}} \begin{Bmatrix} \mathbf{d_1}(z) \\ \mathbf{d_2}(z) \\ \mathbf{d_3}(z) \end{Bmatrix} dz + D_1 \tag{7}$$

in which the following compliance matrices have been defined

$$\begin{aligned} \left[\mathbf{C_{11}}\right]_{3(m+1)\times 3(m+1)} &= (1/E_z)\int_A \hat{\boldsymbol{\chi}}(y)_{3(m+1)\times 1}\,\hat{\boldsymbol{\chi}}(y)^{\mathbf{T}}_{1\times 3(m+1)}\,dA; \\ \left[\mathbf{C_{22}}\right]_{m\times m} &= (1/E_y)\int_A \boldsymbol{\xi}_3(y)_{m\times 1}\,\boldsymbol{\xi}_3(y)^{\mathbf{T}}_{1\times m}\,dA; \\ \left[\mathbf{C_{12}}\right]_{3(m+1)\times m} &= (\mu_{zy}/E_z)\int_A \hat{\boldsymbol{\chi}}(y)_{3(m+1)\times 1}\,\boldsymbol{\xi}_3(y)^{\mathbf{T}}_{1\times m}\,dA; \\ \left[\mathbf{C_{33}}\right]_{(2m+1)\times(2m+1)} &= (1/G)\int_A \tilde{\boldsymbol{\chi}}(y)_{(2m+1)\times 1}\,\tilde{\boldsymbol{\chi}}(y)^{\mathbf{T}}_{1\times(2m+1)}\,dA; \end{aligned} \tag{8}$$

In Eq. (7), the term $D_1 = \int_L\int_A \left(\sigma_z^{*2}/2E_z + \sigma_y^{*2}/2E_y - \mu_{yz}\sigma_z^*\sigma_y^*/E_z + \tau^{*2}/2G\right)dAdz$ will vanish after taking the variation of the expression, and the traction-dependent displacement vectors are defined as

$$\begin{aligned} \mathbf{d_1}(z)_{3(m+1)\times 1} &= (1/E_z)\int_A \hat{\boldsymbol{\chi}}(y)_{3(m+1)\times 1}\left[\sigma_z^*(y,z) - \mu_{zy}\sigma_y^*(y,z)\right]dA; \\ \mathbf{d_2}(z)_{m\times 1} &= (1/E_y)\int_A \boldsymbol{\xi}_3(y)_{m\times 1}\left[\sigma_y^*(y,z) - \mu_{yz}\sigma_z^*(y,z)\right]dA; \\ \mathbf{d_3}(z)_{(2m+1)\times 1} &= (1/G)\int_A \tilde{\boldsymbol{\chi}}(y)_{(2m+1)\times 1}\,\tau^*(y,z)\,dA; \end{aligned} \tag{9a-c}$$

The load potential energy is the surface integral of the tractions and line loads by the corresponding displacements and is given by

$$\begin{aligned} V^* = \quad & \int_{A_{0\sigma}} w(y,0)\bar{\sigma}_z(y,0)\,dA + \int_{A_{0w}} \bar{w}(y,0)\sigma_z(y,0)\,dA + \int_{A_{0\tau}} v(y,0)\bar{\tau}(y,0)\,dA \\ & + \int_{A_{0v}} \bar{v}(y,0)\tau(y,0)\,dA - \int_{A_{L\sigma}} w(y,L)\bar{\sigma}_z(y,L)\,dA - \int_{A_{Lw}} \bar{w}(y,L)\sigma_z(y,L)\,dA \\ & - \int_{A_{L\tau}} v(y,L)\bar{\tau}(y,L)\,dA_s - \int_{A_{Lv}} \bar{v}(y,L)\tau(y,L)\,dA - \int_L q_y(z)v(z)\,dz - \int_L q_z(z)w(z)\,dz \end{aligned} \tag{10}$$

where all bars denote specified quantities. For example, at end $z_e = 0$, $\overline{\sigma}_z(y,0)$ is the specified longitudinal traction acting on area $A_{0\sigma}$ (Figure 1) and $\overline{w}(y,0)$ is the specified longitudinal displacement acting on area $A_{0w} = A - A_{0\sigma}$. Also, $\overline{\tau}(y,0)$ is the specified shear traction acting on area $A_{0\tau}$ and $\overline{v}(y,0)$ is the specified transverse displacement acting on $A_{0v} = A - A_{0\tau}$, and a similar notation is adopted for end $z_e = L$. In the last two terms of Eq. (10), $q_y(z)$ and $q_z(z)$ are line loads in the transverse and longitudinal directions acting at height $y = a$ (Figure 2). They can be expressed as body forces $p_y(y,z)$ and $p_z(y,z)$ through the Dirac delta function as $q_y(z) = Ap_y(y,z)Dirac(y-a)$ and $q_z(z) = Ap_z(y,z)Dirac(y-a)$ where A is the cross-section area of the beam.

4.2. Variation of total complementary strain energy

From Eqs. (8) and (9), by substituting into Eq. (7), taking the variation of the total complementary internal strain energy $\pi^* = U^* + V^*$, and integrating by parts (Pham 2018), one obtains

$$
\begin{aligned}
&\delta U^* = \\
&= \int_L \delta\mathbf{F}(z)^{\mathrm{T}} \left\{ \hat{\mathbf{I}}_1 \left[\mathbf{C}_{11}\hat{\mathbf{F}}(z) - \mathbf{C}_{12}\mathbf{F}''(z) + \mathbf{d}_1(\mathbf{z}) \right] - \mathbf{C}_{12}^{\mathrm{T}}\hat{\mathbf{F}}''(z) + \mathbf{C}_{22}\mathbf{F}''''(z) + \mathbf{d}_2''(\mathbf{z}) - \tilde{\mathbf{I}}_1\mathbf{C}_{33}\tilde{\mathbf{F}}'(z) - \tilde{\mathbf{I}}_1\mathbf{d}_3'(\mathbf{z}) \right\} dz \\
&+ \delta\mathbf{F}(0)^{\mathrm{T}} \left\{ \int_L \hat{\mathbf{I}}_2 \left[\mathbf{C}_{11}\hat{\mathbf{F}}(z) - \mathbf{C}_{12}\mathbf{F}''(z) + \mathbf{d}_1(\mathbf{z}) \right] dz - \mathbf{C}_{12}^{\mathrm{T}}\hat{\mathbf{F}}'(0) + \mathbf{C}_{22}\mathbf{F}'''(0) + \mathbf{d}_2'(0) - \tilde{\mathbf{I}}_1\mathbf{C}_{33}\tilde{\mathbf{F}}(0) - \tilde{\mathbf{I}}_1\mathbf{d}_3(0) \right\} \\
&+ \delta\mathbf{F}'(0)^{\mathrm{T}} \left\{ \int_L z\hat{\mathbf{I}}_3 \left[\mathbf{C}_{11}\hat{\mathbf{F}}(z) - \mathbf{C}_{12}\mathbf{F}''(z) + \mathbf{d}_1(\mathbf{z}) \right] dz - \left[-\mathbf{C}_{12}^{\mathrm{T}}\hat{\mathbf{F}}(0) + \mathbf{C}_{22}\mathbf{F}''(0) + \mathbf{d}_2(0) \right] + \int_L \tilde{\mathbf{I}}_2 \left[\mathbf{C}_{33}\tilde{\mathbf{F}}(z) + \mathbf{d}_3(\mathbf{z}) \right] dz \right\} \\
&- \delta\mathbf{F}(L)^{\mathrm{T}} \left\{ -\mathbf{C}_{12}^{\mathrm{T}}\hat{\mathbf{F}}'(L) + \mathbf{C}_{22}\mathbf{F}'''(L) - \tilde{\mathbf{I}}_1\mathbf{C}_{33}\tilde{\mathbf{F}}(L) + \mathbf{d}_2'(L) - \tilde{\mathbf{I}}_1\mathbf{d}_3(L) \right\} + \delta\mathbf{F}'(L)^{\mathrm{T}} \left\{ -\mathbf{C}_{12}^{\mathrm{T}}\hat{\mathbf{F}}(L) + \mathbf{C}_{22}\mathbf{F}''(L) + \mathbf{d}_2(L) \right\} \\
&+ \delta N(0) \int_L \hat{\mathbf{I}}_4 \left[\mathbf{C}_{11}\hat{\mathbf{F}}(z) - \mathbf{C}_{12}\mathbf{F}''(z) + \mathbf{d}_1(\mathbf{z}) \right] dz + \delta M(0) \int_L \hat{\mathbf{I}}_6 \left[\mathbf{C}_{11}\hat{\mathbf{F}}(z) - \mathbf{C}_{12}\mathbf{F}''(z) + \mathbf{d}_1(\mathbf{z}) \right] dz + \\
&+ \delta Q(0) \int_L \left[z\hat{\mathbf{I}}_5\mathbf{C}_{11}\hat{\mathbf{F}}(z) - z\hat{\mathbf{I}}_5\mathbf{C}_{12}\mathbf{F}''(z) + \tilde{\mathbf{I}}_3\mathbf{C}_{33}\tilde{\mathbf{F}}(z) + z\hat{\mathbf{I}}_5\mathbf{d}_1(\mathbf{z}) + \tilde{\mathbf{I}}_3\mathbf{d}_3(\mathbf{z}) \right] dz
\end{aligned}
\tag{11}
$$

In Eq.(11), the following matrices have been introduced

$$
\begin{aligned}
&\left[\hat{\mathbf{I}}_1\right]_{m\times 3(m+1)} = \left[[\mathbf{I}]_{m\times m} \mid \mathbf{0}_{m\times m} \mid \mathbf{0}_{m\times m} \mid \mathbf{0}_{m\times 1} \mid \mathbf{0}_{m\times 1} \mid \mathbf{0}_{m\times 1} \right]; \quad \left[\hat{\mathbf{I}}_2\right]_{m\times 3(m+1)} = \left[\mathbf{0}_{m\times m} \mid [\mathbf{I}]_{m\times m} \mid \mathbf{0}_{m\times m} \mid \mathbf{0}_{m\times 1} \mid \mathbf{0}_{m\times 1} \mid \mathbf{0}_{m\times 1} \right]; \\
&\left[\hat{\mathbf{I}}_3\right]_{m\times 3(m+1)} = \left[\mathbf{0}_{m\times m} \mid \mathbf{0}_{m\times m} \mid [\mathbf{I}]_{m\times m} \mid \mathbf{0}_{m\times 1} \mid \mathbf{0}_{m\times 1} \mid \mathbf{0}_{m\times 1} \right]; \quad \left[\hat{\mathbf{I}}_4\right]_{1\times 3(m+1)} = \left[\mathbf{0}_{1\times m} \mid \mathbf{0}_{1\times m} \mid \mathbf{0}_{1\times m} \mid 1 \mid 0 \mid 0 \right]; \\
&\left[\hat{\mathbf{I}}_5\right]_{1\times 3(m+1)} = \left[\mathbf{0}_{1\times m} \mid \mathbf{0}_{1\times m} \mid \mathbf{0}_{1\times m} \mid 0 \mid 1 \mid 0 \right]; \quad \left[\hat{\mathbf{I}}_6\right]_{1\times 3(m+1)} = \left[\mathbf{0}_{1\times m} \mid \mathbf{0}_{1\times m} \mid \mathbf{0}_{1\times m} \mid 0 \mid 0 \mid 1 \right]; \\
&\left[\tilde{\mathbf{I}}_1\right]_{m\times(2m+1)} = \left[\mathbf{I}_{m\times m} \quad \mathbf{0}_{m\times m} \quad \mathbf{0}_{m\times 1} \right]; \quad \left[\tilde{\mathbf{I}}_2\right]_{m\times(2m+1)} = \left[\mathbf{0}_{m\times m} \quad \mathbf{I}_{m\times m} \quad \mathbf{0}_{m\times 1} \right]; \quad \left[\tilde{\mathbf{I}}_3\right]_{1\times(2m+1)} = \left[\mathbf{0}_{1\times m} \quad \mathbf{0}_{1\times m} \quad 1 \right]
\end{aligned}
\tag{12}
$$

The terms $[\mathbf{I}]$ appearing in Eq. (12) denote the identity matrices. By taking the variation of Eq. (10) and noting that the variation of specified tractions and loads vanish, one obtains

$$
\delta V^* = \int_{A_{0w}} \overline{w}(y,0)\delta\sigma_z(y,0)dA + \int_{A_{0v}} \overline{v}(y,0)\delta\tau(y,0)dA - \int_{A_{Lw}} \overline{w}(y,L)\delta\sigma_z(y,L)dA - \int_{A_{Lv}} \overline{v}(y,L)\delta\tau(y,L)dA \tag{13}
$$

Specified displacements $\overline{w}\left(y,z_e\right)$ and $\overline{v}\left(y,z_e\right)$ at member ends $z_e=0,L$, are assumed to follow the distributions $\overline{w}\left(z_e,y\right)=\overline{W}\left(z_e\right)+\overline{\theta}\left(z_e\right)y$ and $\overline{v}\left(z_e,y\right)=\overline{V}\left(z_e\right)$ in which $\overline{W}\left(z_e\right),\overline{V}\left(z_e\right)$ are the specified longitudinal and transverse displacements and $\overline{\theta}\left(z_e\right)$ is the specified rotation (Figure 2) at both beam ends $\left(z_e=0,L\right)$. By substitution into Eq. (13), one obtains

$$\delta V^*=\overline{W}\left(0\right)\delta N\left(0\right)+\overline{V}\left(0\right)\delta Q\left(0\right)+\overline{\theta}\left(0\right)\delta M\left(0\right)-\overline{W}\left(L\right)\delta N\left(L\right)-\overline{V}\left(L\right)\delta Q\left(L\right)-\overline{\theta}\left(L\right)\delta M\left(L\right) \tag{14}$$

in which stress resultants $N\left(z_e\right),Q\left(z_e\right),M\left(z_e\right)$ have been defined in Eq. (4).

Figure 2 Sign convention for (a) Resultant line loads and stress resultants and (b) End displacements

From Eqs. (3a-b), by substituting into Eq.(4), and setting $z=L$, one has

$$\begin{aligned}
N\left(L\right)&=\left[\int_{A_{Lw}}\hat{\boldsymbol{\chi}}\left(y\right)_{1\times3\left(m+1\right)}^{\mathbf{T}}dA\right]\hat{\mathbf{F}}\left(L\right)_{3\left(m+1\right)\times1}+\int_{A_{Lw}}\sigma_z^*\left(y,L\right)dA\\
M\left(L\right)&=\left[\int_{A_{Lw}}y\hat{\boldsymbol{\chi}}\left(y\right)_{1\times3\left(m+1\right)}^{\mathbf{T}}dA\right]\hat{\mathbf{F}}\left(L\right)_{3\left(m+1\right)\times1}+\int_{A_{Lw}}y\sigma_z^*\left(y,L\right)dA\\
Q\left(L\right)&=\left[\int_{A_{L\tau}}\tilde{\boldsymbol{\chi}}\left(y\right)_{1\times\left(2m+1\right)}^{\mathbf{T}}dA\right]\tilde{\mathbf{F}}\left(L\right)_{\left(2m+1\right)\times1}+\int_{A_{L\tau}}\tau^*\left(y,L\right)dA
\end{aligned} \tag{15}$$

By taking the variation of Eq.(15), substituting into Eq.(14) and noting that the variations of the specified tractions and loads vanish (Pham 2018), one obtains

$$\begin{aligned}
\delta V^*=&-\delta\mathbf{F}\left(0\right)^{\mathbf{T}}\left[\left\{\mathbf{a}_1\right\}_{m\times1}\overline{W}\left(L\right)+\left\{\mathbf{a}_2\right\}_{m\times1}\overline{\theta}\left(L\right)\right]-\delta\mathbf{F}'\left(0\right)^{\mathbf{T}}\left[\left\{\mathbf{a}_3\right\}_{m\times1}\overline{W}\left(L\right)+\left\{\mathbf{a}_4\right\}_{m\times1}\overline{V}\left(L\right)+\left\{\mathbf{a}_5\right\}_{m\times1}\overline{\theta}\left(L\right)\right]\\
&-\delta\mathbf{F}\left(L\right)^{\mathbf{T}}\left[\left\{\mathbf{a}_6\right\}_{m\times1}\overline{W}\left(L\right)+\left\{\mathbf{a}_7\right\}_{m\times1}\overline{\theta}\left(L\right)\right]-\delta\mathbf{F}'\left(L\right)^{\mathbf{T}}\left\{\mathbf{a}_8\right\}_{m\times1}\overline{V}\left(L\right)-\delta N\left(0\right)\left[-\overline{W}\left(0\right)+a_9\overline{W}\left(L\right)+a_{10}\overline{\theta}\left(L\right)\right]\\
&-\delta Q\left(0\right)\left[-\overline{V}\left(0\right)+a_{11}\left(L\right)\overline{W}\left(L\right)+a_{12}\left(L\right)\overline{V}\left(L\right)+a_{13}\left(L\right)\overline{\theta}\left(L\right)\right]-\delta M\left(0\right)\left[-\overline{\theta}\left(0\right)+a_{14}\overline{W}\left(L\right)+a_{15}\overline{\theta}\left(L\right)\right]
\end{aligned} \tag{16}$$

in which

$$\begin{aligned}
&\left\{\mathbf{a}_1\right\}_{m\times1}=\int_{A_{Lw}}\left\langle\boldsymbol{\psi}_2\left(y\right)\right\rangle_{1\times m}^{T}dA; && \left\{\mathbf{a}_2\right\}_{m\times1}=\int_{A_{Lw}}y\left\langle\boldsymbol{\psi}_2\left(y\right)\right\rangle_{1\times m}^{T}dA;\\
&\left\{\mathbf{a}_3\right\}_{m\times1}=L\int_{A_{Lw}}\left\langle\boldsymbol{\psi}_1\left(y\right)\right\rangle_{1\times m}^{T}dA; && \left\{\mathbf{a}_4\right\}_{m\times1}=\int_{A_{L\tau}}\left\langle\boldsymbol{\psi}_3\left(y\right)\right\rangle_{1\times m}^{T}dA;\\
&\left\{\mathbf{a}_5\right\}_{m\times1}=L\int_{A_{Lw}}y\left\langle\boldsymbol{\psi}_1\left(y\right)\right\rangle_{1\times m}^{T}dA; && \left\{\mathbf{a}_6\right\}_{m\times1}=\int_{A_{Lw}}\left\langle\boldsymbol{\xi}_1\left(y\right)\right\rangle_{1\times m}^{T}dA;\\
&\left\{\mathbf{a}_7\right\}_{m\times1}=\int_{A_{Lw}}y\left\langle\boldsymbol{\xi}_1\left(y\right)\right\rangle_{1\times m}^{T}dA; && \left\{\mathbf{a}_8\right\}_{m\times1}=\int_{A_{L\tau}}\left\langle\boldsymbol{\xi}_2\left(y\right)\right\rangle_{1\times m}^{T}dA;\\
&a_9=\int_{A_{Lw}}\eta_{12}\left(y\right)dA=1; && a_{10}=\int_{A_{Lw}}y\eta_{12}\left(y\right)dA=0; && a_{11}\left(L\right)=\int_{A_{Lw}}L\eta_{13}\left(y\right)dA=0;\\
&a_{12}\left(L\right)=\int_{A_{L\tau}}\eta_{22}\left(y,L\right)dA=1; && a_{14}=\int_{A_{Lw}}\eta_{14}\left(y\right)dA=0; && a_{15}=\int_{A_{Lw}}y\eta_{14}\left(y\right)dA=1;\\
&a_{13}\left(L\right)=\left[L/b\left(h_2\right)\right]\left\{\left[\int_{-h_1}^{h_2}b\left(y\right)y^{n-1}dy\right]^2-\left[\int_{-h_1}^{h_2}b\left(y\right)y^{n}dy\right]\left[\int_{-h_1}^{h_2}b\left(y\right)y^{n-2}dy\right]\right\}
\end{aligned} \tag{17}$$

4.3. Compatibility equations and boundary conditions

From Eqs. (11) and (16), by substituting into the stationarity condition $\delta\pi^* = \delta U^* + \delta V^* = 0$, one obtains m compatibility equations:

$$\mathbf{C}_{22}\mathbf{F}''''(z) - \left[\hat{\mathbf{I}}_1\mathbf{C}_{12} + \mathbf{C}_{12}^{\mathrm{T}}\hat{\mathbf{I}}_1^{\mathrm{T}} + \tilde{\mathbf{I}}_1\mathbf{C}_{33}\tilde{\mathbf{I}}_1^{\mathrm{T}}\right]\mathbf{F}''(z) + \hat{\mathbf{I}}_1\mathbf{C}_{11}\hat{\mathbf{I}}_1^{\mathrm{T}}\mathbf{F}(z) = \mathbf{R}_{\mathrm{p}1}(z) + \mathbf{R}_{\mathrm{p}2}(z) \tag{18}$$

in which $\mathbf{R}_{\mathrm{p}1}(z) = -\hat{\mathbf{I}}_1\mathbf{C}_{11}\hat{\mathbf{I}}_2^{\mathrm{T}}\mathbf{F}(0) - z\hat{\mathbf{I}}_1\mathbf{C}_{11}\hat{\mathbf{I}}_3^{\mathrm{T}}\mathbf{F}'(0) - \hat{\mathbf{I}}_1\mathbf{C}_{11}\hat{\mathbf{I}}_4^{\mathrm{T}}N(0) - z\hat{\mathbf{I}}_1\mathbf{C}_{11}\hat{\mathbf{I}}_5^{\mathrm{T}}Q(0) - \hat{\mathbf{I}}_1\mathbf{C}_{11}\hat{\mathbf{I}}_6^{\mathrm{T}}M(0)$ and $\mathbf{R}_{\mathrm{p}2}(z) = -\hat{\mathbf{I}}_1\mathbf{d}_1(z) - \mathbf{d}_2''(z) + \tilde{\mathbf{I}}_1\mathbf{d}_3'(z) = 0$. The corresponding $4m+3$ boundary conditions are obtained as

$$\begin{aligned}
&\delta\mathbf{F}(0)^{\mathrm{T}}\left\{\int_0^L\left[\hat{\mathbf{I}}_2\mathbf{C}_{11}\hat{\mathbf{I}}_1^{\mathrm{T}}\mathbf{F}(z) - \hat{\mathbf{I}}_2\mathbf{C}_{12}\mathbf{F}''(z)\right]dz + \int_0^L\left[\hat{\mathbf{I}}_2\mathbf{C}_{11}\hat{\mathbf{I}}_2^{\mathrm{T}}\mathbf{F}(0) + \hat{\mathbf{I}}_2\mathbf{C}_{11}\hat{\mathbf{I}}_3^{\mathrm{T}}z\mathbf{F}'(0)\right]dz\right.\\
&\quad + \mathbf{C}_{22}\mathbf{F}'''(0) - \mathbf{C}_{12}^{\mathrm{T}}\hat{\mathbf{I}}_1^{\mathrm{T}}\mathbf{F}'(0) - \mathbf{C}_{12}^{\mathrm{T}}\hat{\mathbf{I}}_3^{\mathrm{T}}\mathbf{F}'(0) - \tilde{\mathbf{I}}_1\mathbf{C}_{33}\tilde{\mathbf{I}}_1^{\mathrm{T}}\mathbf{F}'(0) - \tilde{\mathbf{I}}_1\mathbf{C}_{33}\tilde{\mathbf{I}}_2^{\mathrm{T}}\mathbf{F}'(0)\\
&\quad + \int_0^L\hat{\mathbf{I}}_2\mathbf{C}_{11}\hat{\mathbf{I}}_4^{\mathrm{T}}N(0)dz + \left[\int_0^L\hat{\mathbf{I}}_2\mathbf{C}_{11}\hat{\mathbf{I}}_5^{\mathrm{T}}zdz - \mathbf{C}_{12}^{\mathrm{T}}\hat{\mathbf{I}}_5^{\mathrm{T}} - \tilde{\mathbf{I}}_1\mathbf{C}_{33}\tilde{\mathbf{I}}_3^{\mathrm{T}}\right]Q(0) + \int_0^L\hat{\mathbf{I}}_2\mathbf{C}_{11}\hat{\mathbf{I}}_6^{\mathrm{T}}M(0)dz\\
&\quad \left. + \int_0^L\hat{\mathbf{I}}_2\mathbf{d}_1(\mathbf{z})dz + \mathbf{d}_2'(0) - \tilde{\mathbf{I}}_1\mathbf{d}_3(0) - \left[\{\mathbf{a}_1\}W(L) + \{\mathbf{a}_2\}\theta(L)\right]\right\} = 0
\end{aligned} \tag{19}$$

$$\begin{aligned}
&\delta\mathbf{F}'(0)^{\mathrm{T}}\left\{\int_0^L\left[z\hat{\mathbf{I}}_3\mathbf{C}_{11}\hat{\mathbf{I}}_1^{\mathrm{T}}\mathbf{F}(z) + \tilde{\mathbf{I}}_2\mathbf{C}_{33}\tilde{\mathbf{I}}_1^{\mathrm{T}}\mathbf{F}'(z) - z\hat{\mathbf{I}}_3\mathbf{C}_{12}\mathbf{F}''(z)\right]dz - \mathbf{C}_{22}\mathbf{F}''(0) + \int_0^L z\hat{\mathbf{I}}_3\mathbf{C}_{11}\hat{\mathbf{I}}_2^{\mathrm{T}}\mathbf{F}(0)dz\right.\\
&\quad + \mathbf{C}_{12}^{\mathrm{T}}\hat{\mathbf{I}}_1^{\mathrm{T}}\mathbf{F}(0) + \mathbf{C}_{12}^{\mathrm{T}}\hat{\mathbf{I}}_2^{\mathrm{T}}\mathbf{F}(0) + \int_0^L\left[z^2\hat{\mathbf{I}}_3\mathbf{C}_{11}\hat{\mathbf{I}}_3^{\mathrm{T}}\mathbf{F}'(0) + \tilde{\mathbf{I}}_2\mathbf{C}_{33}\tilde{\mathbf{I}}_2^{\mathrm{T}}\mathbf{F}'(0)\right]dz + \int_0^L z\hat{\mathbf{I}}_3\mathbf{C}_{11}\hat{\mathbf{I}}_4^{\mathrm{T}}N(0)dz\\
&\quad + \mathbf{C}_{12}^{\mathrm{T}}\hat{\mathbf{I}}_4^{\mathrm{T}}N(0) + \int_0^L\left[z^2\hat{\mathbf{I}}_3\mathbf{C}_{11}\hat{\mathbf{I}}_5^{\mathrm{T}} + \tilde{\mathbf{I}}_2\mathbf{C}_{33}\tilde{\mathbf{I}}_3^{\mathrm{T}}\right]Q(0)dz + \int_0^L z\hat{\mathbf{I}}_3\mathbf{C}_{11}\hat{\mathbf{I}}_6^{\mathrm{T}}M(0)dz + \mathbf{C}_{12}^{\mathrm{T}}\hat{\mathbf{I}}_6^{\mathrm{T}}M(0)\\
&\quad \left. + \int_0^L z\hat{\mathbf{I}}_3\mathbf{d}_1(\mathbf{z})dz - \mathbf{d}_2(0) + \int_0^L\tilde{\mathbf{I}}_2\mathbf{d}_3(\mathbf{z})dz - \left[\{\mathbf{a}_3\}W(L) + \{\mathbf{a}_4\}V(L) + \{\mathbf{a}_5\}\theta(L)\right]\right\} = 0
\end{aligned} \tag{20}$$

$$\begin{aligned}
&\delta\mathbf{F}(L)^{\mathrm{T}}\left\{-\mathbf{C}_{12}^{\mathrm{T}}\hat{\mathbf{I}}_1^{\mathrm{T}}\mathbf{F}'(L) - \tilde{\mathbf{I}}_1\mathbf{C}_{33}\tilde{\mathbf{I}}_1^{\mathrm{T}}\mathbf{F}'(L) + \mathbf{C}_{22}\mathbf{F}'''(L) - \mathbf{C}_{12}^{\mathrm{T}}\hat{\mathbf{I}}_3^{\mathrm{T}}\mathbf{F}'(0) - \tilde{\mathbf{I}}_1\mathbf{C}_{33}\tilde{\mathbf{I}}_2^{\mathrm{T}}\mathbf{F}'(0)\right.\\
&\quad \left. - \mathbf{C}_{12}^{\mathrm{T}}\hat{\mathbf{I}}_5^{\mathrm{T}}Q(0) - \tilde{\mathbf{I}}_1\mathbf{C}_{33}\tilde{\mathbf{I}}_3^{\mathrm{T}}Q(0) + \mathbf{d}_2'(L) - \tilde{\mathbf{I}}_1\mathbf{d}_3(L) + \left[\{\mathbf{a}_6\}_{n-2,1}W(L) + \{\mathbf{a}_7\}_{n-2,1}\theta(L)\right]\right\} = 0
\end{aligned} \tag{21}$$

$$\begin{aligned}
&\delta\mathbf{F}'(L)^{\mathrm{T}}\left\{-\mathbf{C}_{12}^{\mathrm{T}}\hat{\mathbf{I}}_1^{\mathrm{T}}\mathbf{F}(L) + \mathbf{C}_{22}\mathbf{F}''(L) - \mathbf{C}_{12}^{\mathrm{T}}\hat{\mathbf{I}}_2^{\mathrm{T}}\mathbf{F}(0) - L\mathbf{C}_{12}^{\mathrm{T}}\hat{\mathbf{I}}_3^{\mathrm{T}}\mathbf{F}'(0) - \mathbf{C}_{12}^{\mathrm{T}}\hat{\mathbf{I}}_4^{\mathrm{T}}N(0)\right.\\
&\quad \left. - L\mathbf{C}_{12}^{\mathrm{T}}\hat{\mathbf{I}}_5^{\mathrm{T}}Q(0) - \mathbf{C}_{12}^{\mathrm{T}}\hat{\mathbf{I}}_6^{\mathrm{T}}M(0) + \mathbf{d}_2(L) - \{\mathbf{a}_8\}_{n-2,1}V(L)\right\} = 0
\end{aligned} \tag{22}$$

$$\begin{aligned}
&\delta N(0)\left\{\int_0^L\left\{\left[\hat{\mathbf{I}}_4\mathbf{C}_{11}\hat{\mathbf{I}}_1^{\mathrm{T}}\mathbf{F}(z) - \hat{\mathbf{I}}_4\mathbf{C}_{12}\mathbf{F}''(z)\right] + \hat{\mathbf{I}}_4\mathbf{C}_{11}\hat{\mathbf{I}}_2^{\mathrm{T}}\mathbf{F}(0) + \hat{\mathbf{I}}_4\mathbf{C}_{11}\hat{\mathbf{I}}_3^{\mathrm{T}}z\mathbf{F}'(0) + \hat{\mathbf{I}}_4\mathbf{C}_{11}\hat{\mathbf{I}}_4^{\mathrm{T}}N(0) + \right.\right.\\
&\quad \left.\left. + \hat{\mathbf{I}}_4\mathbf{C}_{11}\hat{\mathbf{I}}_5^{\mathrm{T}}zQ(0) + \hat{\mathbf{I}}_4\mathbf{C}_{11}\hat{\mathbf{I}}_6^{\mathrm{T}}M(0) + \hat{\mathbf{I}}_4\mathbf{d}_1(\mathbf{z})\right\}dz - \left[W(0) + W(L)\right]\right\} = 0
\end{aligned} \tag{23}$$

$$\delta Q(0)\Big\{\int_0^L\Big[z\hat{\mathbf{I}}_5\mathbf{C}_{11}\hat{\mathbf{I}}_1^{\mathrm{T}}\mathbf{F}(z)+\tilde{\mathbf{I}}_3\mathbf{C}_{33}\tilde{\mathbf{I}}_1^{\mathrm{T}}\mathbf{F}'(z)-z\hat{\mathbf{I}}_5\mathbf{C}_{12}\mathbf{F}''(z)+z\hat{\mathbf{I}}_5\mathbf{C}_{11}\hat{\mathbf{I}}_2^{\mathrm{T}}\mathbf{F}(0)+z^2\hat{\mathbf{I}}_5\mathbf{C}_{11}\hat{\mathbf{I}}_3^{\mathrm{T}}\mathbf{F}'(0)+\tilde{\mathbf{I}}_3\mathbf{C}_{33}\tilde{\mathbf{I}}_2^{\mathrm{T}}\mathbf{F}'(0)$$
$$+z\hat{\mathbf{I}}_5\mathbf{C}_{11}\hat{\mathbf{I}}_4^{\mathrm{T}}N(0)+z^2\hat{\mathbf{I}}_5\mathbf{C}_{11}\hat{\mathbf{I}}_5^{\mathrm{T}}Q(0)+\tilde{\mathbf{I}}_3\mathbf{C}_{33}\tilde{\mathbf{I}}_3^{\mathrm{T}}Q(0)+z\hat{\mathbf{I}}_5\mathbf{C}_{11}\hat{\mathbf{I}}_6^{\mathrm{T}}M(0)+z\hat{\mathbf{I}}_5\mathbf{d}_1(\mathbf{z})+\tilde{\mathbf{I}}_3\mathbf{d}_3(\mathbf{z})\Big]dz \tag{24}$$
$$-\big[V(0)+V(L)+a_{13}\theta(L)\big]\Big\}=0$$

$$\delta M(0)\Big\{\int_0^L\Big[\hat{\mathbf{I}}_6\mathbf{C}_{11}\hat{\mathbf{I}}_1^{\mathrm{T}}\mathbf{F}(z)-\hat{\mathbf{I}}_6\mathbf{C}_{12}\mathbf{F}''(z)+\hat{\mathbf{I}}_6\mathbf{C}_{11}\hat{\mathbf{I}}_2^{\mathrm{T}}\mathbf{F}(0)+z\hat{\mathbf{I}}_6\mathbf{C}_{11}\hat{\mathbf{I}}_3^{\mathrm{T}}\mathbf{F}'(0)+\hat{\mathbf{I}}_6\mathbf{C}_{11}\hat{\mathbf{I}}_4^{\mathrm{T}}N(0)$$
$$+z\hat{\mathbf{I}}_6\mathbf{C}_{11}\hat{\mathbf{I}}_5^{\mathrm{T}}Q(0)+\hat{\mathbf{I}}_6\mathbf{C}_{11}\hat{\mathbf{I}}_6^{\mathrm{T}}M(0)+\hat{\mathbf{I}}_6\mathbf{d}_1(\mathbf{z})\Big]dz-\big[-\theta(0)+\theta(L)\big]\Big\}=0 \tag{25}$$

The m compatibility equations in Eq. (18) are of the fourth order and their integration leads to $4m$ unknown integration constants. The boundary conditions(19)-(25) involve nine end variables $W(0),V(0),\theta(0),W(L),$ $V(L),\theta(L),N(0),Q(0),M(0)$ of which six will be known a-priori in a given problem. Thus, the total number of unknown constants is $4m+3$. In Eqs. (19)-(25), either the variations $\delta\mathbf{F}(0)^{\mathbf{T}}$, $\delta\mathbf{F}'(0)^{\mathbf{T}}$, $\delta\mathbf{F}(L)^{\mathbf{T}}$ and $\delta\mathbf{F}'(L)^{\mathbf{T}}$ or the corresponding bracketed terms will vanish, leading to $4m$ boundary equations. It is always possible to select the z orientation so that either $\delta N(0)$, $\delta Q(0)$ or $\delta M(0)$ or the corresponding bracketed terms vanish, leading to three additional equations and bringing the total number of boundary equations to $4m+3$. Explicit expressions of the stresses, field equations, boundary conditions, and solutions for simple beams are provided in Example 1.

4.3. Closed form solution

The homogeneous solution of the system is obtained by setting $\mathbf{R}_{\mathbf{p1}}(z)+\mathbf{R}_{\mathbf{p2}}(z)=\mathbf{0}$ in Eqs. (18) and is assumed to take the form $\{\mathbf{F}_H(z)\}_{m\times1}=\sum\{\mathbf{F}_{Hi}(z)\}_{m\times1}$ where $\{\mathbf{F}_{Hi}(z)\}_{m\times1}=\{\phi_i\}_{m\times1}e^{c_iz}A_i$, $\{\phi_i\}=\langle 1 \quad \phi_{2,i} \quad \dots \quad \phi_{m,i}\rangle$, in which A_i are unknown constants and c_i depends on the eigen-solution of the compatibility equations.

By substituting $\{\mathbf{F}_{Hi}(z)\}_{m\times1}$ into Eq. (18), one obtains $\Big[c_i^4\mathbf{C}_{22}-\Big(\hat{\mathbf{I}}_1\mathbf{C}_{12}+\mathbf{C}_{12}^{\mathrm{T}}\hat{\mathbf{I}}_1^{\mathrm{T}}+\tilde{\mathbf{I}}_1\mathbf{C}_{33}\tilde{\mathbf{I}}_1^{\mathrm{T}}\Big)c_i^2+\hat{\mathbf{I}}_1\mathbf{C}_{11}\hat{\mathbf{I}}_1^{\mathrm{T}}\Big]_{m\times m}\{\phi_i\}_{m\times1}A_i=0$. For a non-trivial solution, the determinant of the matrix of coefficients vanishes. Given that the resulting eigenvalue problem is quartic in constant c_i, one obtains $4m$ eigen-pairs and the resulting solution takes the form

$$\{\mathbf{F_H}(z)\}_{m\times1}=\{\mathbf{f}\}_{m\times4m}\big[\mathbf{e}(z)\big]_{4m\times4m}\{\mathbf{A}\}_{4m\times1} \tag{26}$$

in which

$$\{\mathbf{f}\}_{m\times4m}=\begin{bmatrix}1&1&\dots&1\\ \phi_{2,1}&\phi_{2,2}&\cdots&\phi_{2,4m}\\ \vdots&\vdots&\ddots&\vdots\\ \phi_{m,1}&\phi_{m,2}&\cdots&\phi_{m,4m}\end{bmatrix};\quad \big[\mathbf{e}(z)\big]_{4m\times4m}=\begin{Bmatrix}e^{c_1z}&0&\dots&0\\ 0&e^{c_2z}&\dots&0\\ \vdots&\vdots&\ddots&\vdots\\ 0&0&\dots&e^{c_{4m}z}\end{Bmatrix};\quad \{\mathbf{A}\}_{4m\times1}=\begin{Bmatrix}A_1\\ A_2\\ \vdots\\ A_{4m}\end{Bmatrix} \tag{27}$$

The particular solution $\{\mathbf{F_{P1}}(z)\}_{m\times1}$ corresponding to $\mathbf{R}_{\mathbf{p1}}(z)$ as given in Eq. (18) is assumed to take the form

$$\left\{\mathbf{F_{P1}}(z)\right\}_{m\times 1}=\left[\overline{\mathbf{C}}_1\right]_{m\times m}\left\{\mathbf{F}(0)\right\}_{m\times 1}+z\left[\overline{\mathbf{C}}_2\right]_{m\times m}\left\{\mathbf{F}'(0)\right\}_{m\times 1}+\left\{\overline{\mathbf{C}}_3\right\}_{m\times 1}N(0)+z\left\{\overline{\mathbf{C}}_4\right\}_{m\times 1}Q(0)+\left\{\overline{\mathbf{C}}_5\right\}_{m\times 1}M(0) \quad (28)$$

From Eq. (28), by substituting into Eq. (18), matrices and vectors $\overline{\mathbf{C}}_1-\overline{\mathbf{C}}_5$ are determined as

$$\left[\overline{\mathbf{C}}_1\right]_{m\times m}=-\left(\hat{\mathbf{I}}_1\mathbf{C}_{11}\hat{\mathbf{I}}_1^{\mathbf{T}}\right)^{-1}\hat{\mathbf{I}}_1\mathbf{C}_{11}\hat{\mathbf{I}}_2^{\mathbf{T}};\qquad \left[\overline{\mathbf{C}}_2\right]_{m\times m}=-\left(\hat{\mathbf{I}}_1\mathbf{C}_{11}\hat{\mathbf{I}}_1^{\mathbf{T}}\right)^{-1}\hat{\mathbf{I}}_1\mathbf{C}_{11}\hat{\mathbf{I}}_3^{\mathbf{T}};$$

$$\left\{\overline{\mathbf{C}}_3\right\}_{m\times 1}=-\left(\hat{\mathbf{I}}_1\mathbf{C}_{11}\hat{\mathbf{I}}_1^{\mathbf{T}}\right)^{-1}\hat{\mathbf{I}}_1\mathbf{C}_{11}\hat{\mathbf{I}}_4^{\mathbf{T}};\qquad \left\{\overline{\mathbf{C}}_4\right\}_{m\times 1}=-\left(\hat{\mathbf{I}}_1\mathbf{C}_{11}\hat{\mathbf{I}}_1^{\mathbf{T}}\right)^{-1}\hat{\mathbf{I}}_1\mathbf{C}_{11}\hat{\mathbf{I}}_5^{\mathbf{T}};\qquad \left\{\overline{\mathbf{C}}_5\right\}_{m\times 1}=-\left(\hat{\mathbf{I}}_1\mathbf{C}_{11}\hat{\mathbf{I}}_1^{\mathbf{T}}\right)^{-1}\hat{\mathbf{I}}_1\mathbf{C}_{11}\hat{\mathbf{I}}_6^{\mathbf{T}}$$

Vector $\mathbf{R_{p2}}(z)$ in Eq. (18) depends upon the applied tractions $\sigma_y(h_1,z)$, $\tau(h_1,z)$, $\sigma_y(h_2,z)$, $\tau(h_2,z)$. The tractions are assumed as a power series with $u+1$ terms, i.e.,

$$\left\langle\sigma_y(h_1,z),\tau(h_1,z),\sigma_y(h_2,z),\tau(h_2,z)\right\rangle=\left\langle\sum_{i=0}^{u}\overline{a}_iz^i,\sum_{i=0}^{u}\overline{b}_iz^i,\sum_{i=0}^{u}\overline{c}_iz^i,\sum_{i=0}^{u}\overline{d}_iz^i\right\rangle \quad (29)$$

where u is the highest power of the series, and $\overline{a}_i,\overline{b}_i,\overline{c}_i,\overline{d}_i$ are known constants.

Vector $\mathbf{R_{p2}}(z)$ can be evaluated from the tractions as given in Eq. (29) through the following four-step procedure:

(1) Substitute the tractions expressions in Eq. (29) into Eq.(54) to obtain $\overline{\tau}(y,z)$ and $\overline{\sigma}_y(y,z)$.

(2) Given the traction expression in Eq. (29) and the expressions for $\overline{\tau}(y,z)$ and $\overline{\sigma}_y(y,z)$, substitute into Eqs. (58) to obtain $\rho_1(z)$ and $\rho_2(z)$.

(3) Given ς_{11} and ς_{21} as determined from Eq. Eq. (56) and $\rho_1(z)$, $\rho_2(z)$ as determined from step 2, determine the load dependent terms $\sigma_z^*(y,z),\tau^*(y,z)$ and $\sigma_y^*(y,z)$ from Eqs.(5)a-c. If the power series in Eq. (29) consists of $u+1$ terms, the double integration with respect to z of Eq. (5)a, increases the power series of $\sigma_z^*(y,z)$ to $u+3$ terms, and

(4) The expressions for $\sigma_z^*(y,z),\tau^*(y,z)$ and $\sigma_y^*(y,z)$ as provided in Appendix 1 are substituted into Eq. (9) to determine $\mathbf{d_1}(z),\mathbf{d_2}(z),\mathbf{d_3}(z)$, and hence vector $\left\{\mathbf{R_{p2}}(z)\right\}$ can be expressed as

$$\left\{\mathbf{R_{p2}}(z)\right\}_{m\times 1}=\left[\mathbf{g}\right]_{m\times(u+3)}\left\{\mathbf{Z}(z)\right\}_{(u+3)\times 1} \quad (30)$$

In Eq. (30), matrix $\left[\mathbf{g}\right]_{m\times(u+3)}$ is known and vector $\left\langle\mathbf{Z}\right\rangle_{1\times(u+3)}^{\mathbf{T}}=\left\langle 1\quad z\quad\ldots\quad z^{u+2}\right\rangle$ has been defined. The particular solution $\left\{\mathbf{F_{P2}}(z)\right\}_{m\times 1}$ corresponding to $\mathbf{R_{p2}}(z)$ can be assumed to take the form

$$\left\{\mathbf{F_{P2}}(z)\right\}_{m\times 1}=\left[\overline{\mathbf{C}}\right]_{m\times(u+3)}\left\{\mathbf{Z}(z)\right\}_{(u+3)\times 1} \quad (31)$$

where $\left[\overline{\mathbf{C}}\right]$ is an unknown matrix. From Eqs. (30), (31), by substituting into Eq. (18), one obtains

$$\mathbf{C}_{22}\left[\overline{\mathbf{C}}\right]_{m\times(u+3)}\left\{\mathbf{Z}_1(z)\right\}''''_{(u+3)\times 1}-\left[\hat{\mathbf{I}}_1\mathbf{C}_{12}+\mathbf{C}_{12}^{\mathrm{T}}\hat{\mathbf{I}}_1^{\mathrm{T}}+\tilde{\mathbf{I}}_1\mathbf{C}_{33}\tilde{\mathbf{I}}_1^{\mathrm{T}}\right]\left[\overline{\mathbf{C}}\right]_{m\times(u+3)}\left\{\mathbf{Z}_1(z)\right\}''_{(u+3)\times 1}+$$
$$+\hat{\mathbf{I}}_1\mathbf{C}_{11}\hat{\mathbf{I}}_1^{\mathrm{T}}\left[\overline{\mathbf{C}}\right]_{m\times(u+3)}\left\{\mathbf{Z}_1(z)\right\}_{(u+3)\times 1}=\left[\overline{\mathbf{A}}\right]_{m\times(u+3)}\left\{\mathbf{Z}(z)\right\}_{(u+3)\times 1} \tag{32}$$

From Eq.(32), by equating the coefficients of z^i on both sides, one recovers the $m\times(u+3)$ equations that relate the coefficients of matrix $[\mathbf{g}]$ to those of the of unknown matrix $\left[\overline{\mathbf{C}}\right]$.

The general solution of Eqs. (18) is obtained by substituting Eq. (27) into Eq. (26), and then summing Eq. (26), (28) and (31) yielding

$$\left\{\mathbf{F}(z)\right\}_{m\times 1}=\left\{\mathbf{f}\right\}_{m\times 4m}\left[\mathbf{e}(z)\right]_{4m\times 4m}\left\{\mathbf{A}\right\}_{4m\times 1}+\left[\overline{\mathbf{C}}_1\right]_{m\times m}\left\{\mathbf{F}(\mathbf{0})\right\}_{m\times 1}+z\left[\overline{\mathbf{C}}_2\right]_{m\times m}\left\{\mathbf{F}'(\mathbf{0})\right\}_{m\times 1}+$$
$$+\left\{\overline{\mathbf{C}}_3\right\}_{m\times 1}N(0)+z\left\{\overline{\mathbf{C}}_4\right\}_{m\times 1}Q(0)+\left\{\overline{\mathbf{C}}_5\right\}_{m\times 1}M(0)+\left[\overline{\mathbf{C}}\right]_{m\times(u+3)}\left\{\mathbf{Z}(z)\right\}_{(u+3)\times 1} \tag{33}$$

By setting $z=0$ in Eq. (33), and noting that $\left[\mathbf{e}(0)\right]=[\mathbf{I}]$, one obtains

$$\left\{\mathbf{F}(0)\right\}_{m,1}=\left\{\mathbf{f}\right\}_{m\times 4m}\left\{\mathbf{A}\right\}_{4m\times 1}+\left[\overline{\mathbf{C}}_1\right]_{m,m}\left\{\mathbf{F}(\mathbf{0})\right\}_{m,1}+\left\{\overline{\mathbf{C}}_3\right\}_{m,1}N(0)+\left\{\overline{\mathbf{C}}_5\right\}_{m,1}M(0)+\left[\overline{\mathbf{C}}\right]_{m,u}\left\{\mathbf{Z}(0)\right\}_{u,1} \tag{34}$$

By solving Eq. (34) for $\left\{\mathbf{F}(\mathbf{0})\right\}$, one obtains

$$\left\{\mathbf{F}(\mathbf{0})\right\}_{m\times 1}=\left[\bar{\mathbf{I}}-\overline{\mathbf{C}}_1\right]_{m\times m}^{-1}\left\{\left\{\mathbf{f}\right\}_{m\times 4m}\left[\mathbf{e}(0)\right]_{4m\times 4m}\left\{\mathbf{A}\right\}_{4m\times 1}+N(0)\left\{\overline{\mathbf{C}}_3\right\}_{m\times 1}+M(0)\left\{\overline{\mathbf{C}}_5\right\}_{m\times 1}+\left[\overline{\mathbf{C}}\right]_{m\times(u+3)}\left\{\mathbf{Z}(0)\right\}_{(u+3)\times 1}\right\} \tag{35}$$

Also, from Eq.(33), by taking the first derivative of both sides with respect to z , setting $z=0$ and solving for $\left\{\mathbf{F}'(0)\right\}_{m\times 1}$, one obtains

$$\left\{\mathbf{F}'(0)\right\}_{m\times 1}=\left[\bar{\mathbf{I}}-\overline{\mathbf{C}}_2\right]_{m\times m}^{-1}\times\left(\left\{\mathbf{f}\right\}_{m\times 4m}\left[\mathbf{e}'(0)\right]_{4m\times 4m}\left\{\mathbf{A}\right\}_{4m\times 1}+Q(0)\left\{\overline{\mathbf{C}}_4\right\}_{m\times 1}+\left[\overline{\mathbf{C}}\right]_{m\times(u+3)}\left\{\mathbf{Z}'(0)\right\}_{(u+3)\times 1}\right) \tag{36}$$

The expressions of $\left\{\mathbf{F}(\mathbf{0})\right\}_{m\times 1}$ and $\left\{\mathbf{F}'(\mathbf{0})\right\}_{m\times 1}$ in Eqs. (35) and (36) are then substituted into Eq. (33) yielding

$$\left\{\mathbf{F}(z)\right\}_{m\times 1}=\left[\mathbf{H}_1(z)\right]_{m\times 4m}\left\{\mathbf{A}\right\}_{4m\times 1}+\left\{\mathbf{H}_2\right\}_{m\times 1}N(0)+z\left\{\mathbf{H}_3\right\}_{m\times 1}Q(0)+\left\{\mathbf{H}_4\right\}_{m\times 1}M(0)+\left\{\mathbf{H}_5(z)\right\}_{m\times 1} \tag{37}$$

in which the following matrices have been defined.

$$\begin{aligned}
\left[\mathbf{H}_1(z)\right]_{m\times 4m}&=\left\{\mathbf{f}\right\}_{m\times 4m}\left[\mathbf{e}(z)\right]_{4m\times 4m}+z\left[\overline{\mathbf{C}}_2\right]_{m\times m}\left[\bar{\mathbf{I}}-\overline{\mathbf{C}}_1\right]_{m\times m}^{-1}\left\{\mathbf{f}\right\}_{m\times 4m}\left[\mathbf{e}'(0)\right]_{4m\times 4m}\\
&\quad+\left[\overline{\mathbf{C}}_1\right]_{m\times m}\left[\bar{\mathbf{I}}-\overline{\mathbf{C}}_1\right]_{m\times m}^{-1}\left\{\mathbf{f}\right\}_{m\times 4m}\\
\left\{\mathbf{H}_2\right\}_{m\times 1}&=\left[\bar{\mathbf{I}}-\overline{\mathbf{C}}_1\right]_{m\times m}^{-1}\left\{\overline{\mathbf{C}}_3\right\}_{m\times 1},\\
\left\{\mathbf{H}_3\right\}_{m\times 1}&=\left[\bar{\mathbf{I}}-\overline{\mathbf{C}}_2\right]_{m\times m}^{-1}\left\{\overline{\mathbf{C}}_4\right\}_{m\times 1},\\
\left\{\mathbf{H}_4\right\}_{m\times 1}&=\left[\bar{\mathbf{I}}-\overline{\mathbf{C}}_1\right]_{m\times m}^{-1}\left\{\overline{\mathbf{C}}_5\right\}_{m\times 1},\\
\left\{\mathbf{H}_5(z)\right\}_{m\times 1}&=\left[\overline{\mathbf{C}}\right]_{m\times(u+3)}\left\{\mathbf{Z}(z)\right\}_{(u+3)\times 1}+z\left[\overline{\mathbf{C}}_2\right]_{m\times m}\left[\bar{\mathbf{I}}-\overline{\mathbf{C}}_2\right]_{m\times m}^{-1}\left[\overline{\mathbf{C}}\right]_{m\times(u+3)}\left\{\mathbf{Z}'(0)\right\}_{(u+3)\times 1}\\
&\quad+\left[\overline{\mathbf{C}}_1\right]_{m\times m}\left[\bar{\mathbf{I}}-\overline{\mathbf{C}}_1\right]_{m\times m}^{-1}\left[\overline{\mathbf{C}}\right]_{m\times(u+3)}\left\{\mathbf{Z}(0)\right\}_{(u+3)\times 1}
\end{aligned} \tag{38}$$

From Eqs. (37), by substituting into the $4m+3$ boundary condition in Eq. (19)-(25), one obtains

$$\delta\mathbf{F}(0)^{\mathrm{T}}\left\{\left[\mathbf{b_{11}}\right]_{m\times 4m}\{\mathbf{A}\}_{4m\times 1}+\{\mathbf{b}_{12}\}_{m\times 1}N(0)+\{\mathbf{b}_{13}\}_{m\times 1}Q(0)+\{\mathbf{b}_{14}\}_{m\times 1}M(0)+\left[\mathbf{L_1}\right]_{m\times 1}-\left[\{\mathbf{a}_1\}_{m\times 1}\overline{W}(L)+\{\mathbf{a}_2\}_{m\times 1}\overline{\theta}(L)\right]\right\}=0 \tag{39}$$

$$\delta\mathbf{F}'(0)^{\mathrm{T}}\left\{\left[\mathbf{b}_{21}\right]_{m\times 4m}\{\mathbf{A}\}_{4m\times 1}+\{\mathbf{b}_{22}\}_{m\times 1}N(0)+\{\mathbf{b}_{23}\}_{m\times 1}Q(0)+\{\mathbf{b}_{24}\}_{m\times 1}M(0)+\{\mathbf{L_2}\}_{m\times 1}-\left[\{\mathbf{a}_3\}_{n-2,1}\overline{W}(L)+\{\mathbf{a}_4\}_{n-2,1}\overline{V}(L)+\{\mathbf{a}_5\}_{n-2,1}\overline{\theta}(L)\right]\right\}=0 \tag{40}$$

$$\delta\mathbf{F}(L)^{\mathrm{T}}\left\{\left[\mathbf{b}_{31}\right]_{m\times 4m}\{\mathbf{A}\}_{4m\times 1}+\{\mathbf{b}_{32}\}_{m\times 1}Q(0)+\{\mathbf{L_3}\}_{m\times 1}+\left[\{\mathbf{a}_6\}_{n-2,1}\overline{W}(L)+\{\mathbf{a}_7\}_{n-2,1}\overline{\theta}(L)\right]\right\}=0 \tag{41}$$

$$\delta\mathbf{F}'(L)^{\mathrm{T}}\left\{\left[\mathbf{b}_{41}\right]_{m\times 4m}\{\mathbf{A}\}_{4m\times 1}+\{\mathbf{b}_{42}\}_{m\times 1}N(0)+\{\mathbf{b}_{43}\}_{m\times 1}Q(0)+\{\mathbf{b}_{44}\}_{m\times 1}M(0)+\{\mathbf{L_4}\}_{m\times 1}-\{\mathbf{a}_8\}_{n-2,1}\overline{V}(L)\right\}=0 \tag{42}$$

$$\delta N(0)\left\{\left[\mathbf{b}_{51}\right]_{m\times 4m}\{\mathbf{A}\}_{4m\times 1}+\{\mathbf{b}_{52}\}_{m\times 1}N(0)+\{\mathbf{b}_{53}\}_{m\times 1}Q(0)+\{\mathbf{b}_{54}\}_{m\times 1}M(0)+\{\mathbf{L_5}\}_{m\times 1}-\left[-\overline{W}(0)+\overline{W}(L)\right]\right\}=0 \tag{43}$$

$$\delta Q(0)\left\{\left[\left[\mathbf{b}_{61}\right]_{m\times 4m}\{\mathbf{A}\}_{4m\times 1}+\{\mathbf{b}_{62}\}_{m\times 1}N(0)+\{\mathbf{b}_{63}\}_{m\times 1}Q(0)+\{\mathbf{b}_{64}\}_{m\times 1}M(0)+\{\mathbf{L_6}\}_{m\times 1}\right]-\left[-\overline{V}(0)+\overline{V}(L)+a_{13}\overline{\theta}(L)\right]\right\}=0 \tag{44}$$

$$\delta M(0)\left\{\left[\left[\mathbf{b}_{71}\right]_{m\times 4m}\{\mathbf{A}\}_{4m\times 1}+\{\mathbf{b}_{72}\}_{m\times 1}N(0)+\{\mathbf{b}_{73}\}_{m\times 1}Q(0)+\{\mathbf{b}_{74}\}_{m\times 1}M(0)+\{\mathbf{L_7}\}_{m\times 1}\right]-\left[-\overline{\theta}(0)+\overline{\theta}(L)\right]\right\}=0 \tag{45}$$

in which matrices $\left[\mathbf{b_{ij}}\right]$, ($i=1,...,7$ and $j=1,2,...,4$) depend solely on mechanical properties and beam cross-section, load vectors $\{\mathbf{L}_i\}_{m\times 1}$ are defined in Appendix 2, and one recalls that vectors $\{\mathbf{a_i}\}_{m\times 1}$ have been defined in Eqs. (17).

5. Examples

5.1. Illustrative examples

5.1.1. Beam under uniform traction - number of terms = 3

This section illustrates the applicability of the present theory for a beam with a rectangular cross-section $b\times h$ and subjected to a uniform traction $\sigma(h_1,z)=\sigma_0$ acting at the top surface while other tractions vanish, i.e., $\tau(h_1,z)=\sigma(h_2,z)=\tau(h_2,z)=0$. Two solutions are provided for a cantilever and for a simply supported beam. The number of stress terms taken is n =3.

Stress fields and governing equations: From Eqs. (4) and (5), by substituting into Eq. (3), the expressions for the stress fields are given as

$$\sigma_z(y,z)=\left(1-\frac{12y^2}{h^2}\right)F_1(z)+\frac{12y}{bh^3}\left[yN(0)+zQ(0)+M(0)\right]+\frac{6yz^2}{h^3}\sigma_0$$

$$\tau_{yz}(y,z)=\left(-y+\frac{4y^3}{h^2}\right)F_1'(z)+6\sigma z\left(\frac{1}{4h}-\frac{y^2}{h^3}\right)+6Q(0)\left(\frac{1}{4bh}-\frac{y^2}{bh^3}\right) \tag{46}$$

$$\sigma_y(y,z)=\left(-\frac{h^2}{16}+\frac{y^2}{2}-\frac{y^4}{h^2}\right)F_1''(z)+\frac{1}{2}\left(1-\frac{3y}{h}+\frac{4y^3}{h^3}\right)\sigma_0$$

In this case, the number of compatibility equations is $m=n-2=1$ and the corresponding differential equation of compatibility as given by Eq.(18) takes the form

$$\frac{bh^5}{630E_y}F_1''''(z)+\left(\frac{4\mu_{zy}bh^3}{105E_z}-\frac{2bh^3}{105G}\right)F_1''(z)+\frac{4bh}{5E_z}F_1(z)-\frac{4}{5E_z}N(0)=0 \tag{47}$$

The integration of Eq. (47) gives four unknown constants. Also, equations(19)-(25) give $4m+3=7$ boundary conditions, which take the form

$$\delta F_1(0)\left[\frac{bh^5}{630E_y}F_1'''(0)+\left(\frac{2\mu_{zy}bh^3}{105E_z}-\frac{2bh^3}{105G}\right)F_1'(0)\right]=0$$

$$\delta F_1'(0)\left[-\frac{bh^5}{630E_y}F_1''(0)-\frac{2\mu_{zy}bh^3}{105G}F_1(0)-\frac{\mu_{zy}h^2}{70E_z}N(0)+\frac{\sigma_0bh^3}{60E_y}\right]=0$$

$$\delta F_1(L)\left[\left(\frac{2\mu_{yz}bh^3}{105E_y}-\frac{2bh^3}{105G}\right)F_1'(L)+\frac{bh^5}{630E_y}F_1'''(L)\right]=0$$

$$\delta F_1'(L)\left[\frac{2\mu_{zy}bh^3}{105E_z}F_1(L)+\frac{bh^5}{630E_y}F_1''(L)+\frac{\mu_{yz}h^2}{70E_y}N(0)-\frac{\sigma_0bh^3}{60E_y}\right]=0 \tag{48a-g}$$

$$\delta N(0)\left\{\int_0^L\left[\frac{4F_1(L)}{5E_z}+\frac{\mu_{yz}h^2}{70E_y}F_1''(L)+\frac{9N(0)}{5E_zhb}-\frac{\mu_{yz}\sigma_0}{2E_y}\right]dz-W(0)-W(L)\right\}=0$$

$$\delta Q(0)\left\{\int_0^L\left[\left(\frac{12z^2}{E_zbh^3}+\frac{6}{5Ghb}\right)Q(0)+\frac{12zM(0)}{E_zbh^3}+\frac{6\sigma_0z^3}{E_zh^3}-\frac{6\mu_{yz}\sigma_0z}{5E_yh}+\frac{6\sigma_0z}{5Gh}\right]dz\right.$$
$$\left.-V(0)-V(L)-L\theta(L)\right\}=0$$

$$\delta M(0)\left\{\int_0^L\left[\frac{12zQ(0)}{E_zbh^3}+\frac{12M(0)}{E_zbh^3}+\frac{6\sigma_0z^2}{E_zh^3}+\frac{6\mu_{yz}\sigma_0}{5E_yh}\right]dz+\theta(0)-\theta(L)\right\}=0$$

In Eq.(48), depending on the boundary conditions, either the bracketed expression or its variational coefficient will vanish. It is emphasized that Eqs. (48) are applicable for general boundary conditions.

Case 1: Cantilever

For a cantilever fixed at $z=0$ and free at $z=L$, one has $V(0)=W(0)=\theta(0)=0$. Since the cantilever is not subjected to axial forces, one has $N(0)=0$. By substituting $N(0)=0$ into Eq.(47), enforcing the boundary conditions $\delta F_1(0)\neq 0$, $\delta F_1'(0)\neq 0$, $\delta F_1(L)=0$, $\delta F_1'(L)=0$, $\delta N(0)\neq 0$, $\delta Q(0)\neq 0$, $\delta M(0)\neq 0$ in Eqs. (48

a,g) and solving for the four integration constants and the three unknown displacements $W(L), V(L), \theta(L)$, one obtains $F_1(z)$ which contributes to a nonlinear distribution of the longitudinal normal stresses across the section depth as evidenced in Eq. (46). Boundary equations (48f-g) are found independent of $F_1(z)$. Thus, the angle of rotation $\theta(L)$ and deflection $V(L)$ at the free end can then be evaluated by setting $Q(0) = -\sigma_0 bL$ and $M(0) = \sigma_0 bL^2/2$ leading to

$$\theta(L) = \frac{\sigma_0 bL^3}{6E_z I} + \frac{6\sigma_0 \mu_{yz} L}{5hE_y}; \qquad V(L) = -\left(\frac{\sigma_0 bL^4}{8E_z I} + \frac{3\sigma_0 L^2}{5hG} + \frac{9\sigma_0 \mu_{yz} L^2}{5hE_y} \right) \tag{49)a,b}$$

The first term of the right hand side of Eq. (49a) and the first two terms of Eq. (49b) coincide with those of the Timoshenko beam solution. Thus, the present study is found to provide higher predictions of beam deflections than does the Timoshenko beam theory.

Case 2: Simply supported beam

If the beam is simply supported at both ends, the normal force vanishes within the member given that there are no axial forces applied. By substituting $N(0) = 0$ into Eq. (47) and applying the boundary conditions $\delta F_1(0) \neq 0$, $\delta F_1'(0) \neq 0$, $\delta F_1(L) \neq 0, \delta F_1'(L) \neq 0, \delta N(0) \neq 0, \delta Q(0) \neq 0$ and solving, the four unknown constants of the closed form solution and the two displacements $W(L), \theta(L)$ can be determined. Also, by setting $Q(0) = -\sigma_0 bL/2$ and $M(0) = 0$, the mid-span deflection $V(L/2)$ can be obtained by integrating Eq. (48f) over half of the span while the end rotation $\theta(L)$ can be obtained by integrating Eq. (48f) over the whole span to yield

$$\theta(L) = \frac{\sigma_0 L^3}{2E_z h^3} + \frac{3\mu_{yz}\sigma_0 L}{5E_y h}; \qquad V(L/2) = \frac{5\sigma_0 L^4}{32E_z h^3} + \frac{3\sigma_0 L^2}{20hG} + \frac{3\mu_{yz}\sigma_0 L^2}{20E_y h} \tag{50)a,b}$$

From Eq.(50)b, by noting that $\mu_{yz}/E_y = \mu_{zy}/E_z$ and assuming that $G = E_z/2(1+\mu_{zy})$, the deflection becomes $V(L/2) = 5\sigma_0 L^4/32E_z h^3 + 3\sigma_0 L^2/10E_z h + 9\mu_{zy}\sigma_0 L^2/20E_z h$. This deflection is higher than that based on the theory of elasticity (e.g., Timoshenko and Goodier 1970), which is $V(L/2) = 5\sigma_0 L^4/32E_z h^3, +3\sigma_0 L^2/10E_z h + 3\mu_{zy}\sigma_0 L^2/16E_z h$, indicating that the present solution converges from above.

5.1.2. Stress Fields and Compatibility Equations - number of stress terms = 4

The expressions for the stress fields are given from Eqs. (4) and (5), by substituting into Eq. (3) yielding

$$\begin{aligned}
\sigma_z(y,z) &= \left(1 - \frac{12y^2}{h^2}\right) F_1(z) + \left(y - \frac{20y^3}{3h^2}\right) F_2(z) + \frac{12y^2}{bh^3} N(0) + \frac{80y^3 z}{bh^5} Q(0) + \frac{80y^3}{bh^5} M(0) + \frac{40y^3 z^2}{h^5}\sigma_0 \\
\tau(y,z) &= \left(-y + \frac{4y^3}{h^2}\right) F_1'(z) + \left(\frac{5y^4}{3h^2} - \frac{y^2}{2} + \frac{h^2}{48}\right) F_2'(z) + \left(\frac{5}{4bh} - \frac{20y^4}{bh^5}\right) Q(0) + \left(\frac{5}{4h} - \frac{20y^4}{h^5}\right) z\sigma_0 \\
\sigma_y(y,z) &= \left(-\frac{y^4}{h^2} + \frac{y^2}{2} - \frac{h^2}{16}\right) F_1''(z) + \left(-\frac{y^5}{3h^2} + \frac{y^3}{6} - \frac{h^2}{48} y\right) F_2''(z) + \left(\frac{4y^5}{h^5} - \frac{5y}{4h} + \frac{1}{2}\right)\sigma_0
\end{aligned} \tag{51}$$

The highest order of y in the longitudinal normal stress field is 3, which is higher than that when $n=3$. Also, the compatibility equations as obtained from Eq.(18) take the form

$$\frac{bh^5}{249480E_y}\begin{bmatrix}396 & 0\\ 0 & h^2\end{bmatrix}\mathbf{F}''''(z)+\frac{2bh^3}{11340}\begin{bmatrix}108 & 0\\ 0 & h^2\end{bmatrix}\left(\frac{2\mu_{yz}}{E_z}-\frac{1}{G}\right)\mathbf{F}''(z)+\frac{bh}{315E_z}\begin{bmatrix}252 & 0\\ 0 & 5h^2\end{bmatrix}\mathbf{F}(z)$$
$$-\frac{4}{5E_z}\begin{Bmatrix}1\\ 0\end{Bmatrix}N(0)-\frac{4z}{21E_z}\begin{Bmatrix}0\\ 1\end{Bmatrix}Q(0)-\frac{4}{21E_z}\begin{Bmatrix}0\\ 1\end{Bmatrix}M(0)+\frac{\sigma_0 b}{378}\left(\frac{h^2}{G}-\frac{\mu_{zy}h^2}{E_y}-\frac{\mu_{yz}h^2}{E_z}+\frac{36z^2}{E_z}\right)\begin{Bmatrix}0\\ 1\end{Bmatrix}=0 \quad (52)$$

In this case, the two compatibility equations $F_1(z)$ and $F_z(z)$ are uncoupled (as the off-diagonal terms vanish). This will generally not be the case. For instance for $n\geq 5$, all compatibility equations happen to be coupled. Also, for a T-section, the equations are coupled for $n\geq 4$.

5.2. Example 2: Simply supported wooden beam under uniform traction

A simply supported rectangular wooden beam is considered (Figure 3). Cross-section dimensions are $b\times h$ = $100\times 200mm$. Wood is assumed to have a longitudinal modulus of elasticity E_z = 11.4 GPa, a transverse modulus of elasticity E_y =1.48 GPa, a shear modulus G =1.24 GPa, and a Poisson's ratio $\mu_{zy}=0.35$. The span L is taken as $3h$ and $10h$ to investigate the cases of deep and shallow beams. The uniform traction σ applied to span $L=3h$ is 4.0 MPa while that applied to span $L=10h$ is 0.4 MPa. Load magnitudes were selected to induce longitudinal stress levels at the extreme fiber that are comparable for both cases as predicted by the Euler-Bernoulli theory. The stress fields obtained from the present solution are compared to those based on the Euler-Bernoulli beam, the Timoshenko beam and the 3D FEA under ABAQUS.

Description of the 3D FEA: The C3D8R element in the ABAQUS library is adopted for the 3D FEA solution. The element is an 8-node brick element with 3 translational degrees of freedom per node with reduced integration. For $L=3h$, a mesh sensitivity study was conducted to obtain the number of elements necessary to achieve convergence and the final mesh selected comprised of 40 elements along the width, 80 elements along the height, and 100 elements along the span. For $L=10h$, the number of elements taken along span was 300 elements.

Figure 3 Simply supported beam under a uniform traction

Mid-span deflection: For a span L=10h, the mid-span deflection predicted by the 3D FEA solution is 11.80mm and is taken as a reference solution for comparison. The deflections predicted by the Euler-Bernoulli is 10.44 mm and that based of the Timoshenko beam theory is 11.28mm, which are 11.2% and 4.4% lower than the 3D FEA. The present study with n=3 is predicts a deflection of 11.89mm, and thus overestimates the deflection by 0.8%. For n=4 or 5, and 11.85mm, the present theory overestimates the deflection by 0.4%. Similar observations were observed for L=3h. In all cases, deflections are found to converge asymptotically from above to those predicted by the 3D FEA solution as the number of stress terms n increases.

Longitudinal normal stresses: Figures 4a-b depict the mid-span longitudinal normal stress profiles for spans L=3h and L=10h as predicted by the present study with n=3 and 4, the Timoshenko beam solution, and the 3D FEA. For the short span L=3h, the stress profile predicted by the present solution with n=4 shows a slightly nonlinear distribution in a manner consistent with the 3D FEA solution. In slight contrast, the solutions based on the Timoshenko and present solution with n=3 show a linear stress profile. The peak stress at the top and bottom fibers predicted by the present solution with n=4 and the 3D FEA solution is 30.4 MPa, while that predicted by the Timoshenko and present solution

with n=3 is 27.0 MPa, a 12.6% difference from the 3D FEA. For the longer span L=10h, the stress profiles predicted by all solutions are linear and essentially coincide.

Transverse shear stress profile: Figures 5a-b provide a comparison of the transverse shear stress profiles at end cross-sections for L=3h and L=10h. As observed, the present solutions with n=3, 4 predict identical stress profiles for both spans. The 3D FEA solution predicts a slightly smaller peak shear stress at mid-height fibers and non-zero stresses at the top and bottom fibers, especially for the span L=3h. Because no external shear tractions are applied to the top and bottom faces, the 3D FEA violates the traction boundary condition at both faces. This finding is characteristic of displacement based finite element formulations which interpolate displacement fields. In contrast, the present solution, which is based on statically admissible stress fields, is able to satisfy in an exact sense the horizontal traction boundary conditions at the top and bottom faces. A Comparison with the parabolic shear stress distribution based on the Euler-Bernoulli solution show that the present solution and FEA predict slightly higher peak shear stresses. Also, shown on the Figures 5a-b are the uniform shear stress distribution consistent with the Timoshenko beam hypothesis, which leads to a violation of the shear traction boundary conditions at the top and bottom faces.

Transverse normal stress profiles at mid-span: Figures 6a-b present the transverse normal stress profiles at mid-span section obtained from the present solution with n=3, 4 and the 3D FEA solution for L=3h and L=10h. As observed, all solutions are in excellent agreement. Both solutions contrast with conventional Euler-Bernoulli and Timoshenko beam solutions which cannot capture the transverse normal stresses.

Transverse normal stress profiles at supports: Figure 7a depicts the transverse normal stress profile at the support section as obtained from the present study with n=3-13 and the 3D FEA solution. The present solution is observed to converge when n=9 as further increase in n does not cause a change in the stress profile. The 3D FEA predicted stress profile has a similar trend but different values from those of the present solution. Unlike the present solution which exactly satisfies the vertical traction boundary conditions at the top and bottom faces, the 3D FEA solution violates the vertical traction conditions at both faces.

Transverse normal stress profiles along the span: Figure 7b depicts the transverse normal stress profiles based on the present solution with n=9 for sections at z = 0, 0.1L-0.5L. Except for the stresses at z = 0 where significant localizations occur at the support, all stress profiles are nearly identical.

Figure 4 Longitudinal stress profiles at mid-span cross-section for spans (a) L=3h and (b) L=10h

Figure 5 Transverse shear stress profiles at support cross-sections for spans (a) L=3h, (b) L=10h

Figure 6 Transverse normal stress profiles at mid-span cross-sections for spans (a) L=3h, (b) L=10h (positive stresses denote tension)

Figure 7 Transverse normal stress profiles for L=3h (a) Effect of the number of terms n (z=0), and (b) Effect of cross-section location Z (n=9)

Effect of shear and transverse normal stresses: In order to investigate the effect of shear deformation and transverse stresses on the mid-span deflection, the beam depth is kept constant and the span is changed so that the span-to-depth ratio is varied from 2 to 14. The ratio PS/EB of the peak deflection based present solution (PS) to that based on the Euler-Bernoulli beam solution (EB) is plotted as a function of the L/h ratio (Figure 8). Overlaid on the figure is the ratio PS/TB of the peak deflection based on present solution (PS) to that based on the Timoshenko beam (TB) solution. Also shown are the ratios of deflections predicted by the 3D FEA to those predicted by the EB solution. The results show excellent agreement between the predictions present solution and the 3D FEA. Since the Timoshenko and present solutions capture the effects of longitudinal normal and shear stresses, but only the present solution captures the effect of normal transverse stress, the PS/TB ratio is indicative of transverse deformation effect on the deflection.

Also, since the shear and the transverse stress effects are captured by the present theory but not in the Euler-Bernoulli beam, the ratio PS/EB can be considered to reflect the combined effect of shear and transverse normal stresses. Finally, the vertical distance in Figure 8 between both curves reflect the effect of shear stresses alone. As expected, shear deformation effects are significant for short spans (e.g., PS/EB-PS/TB=3.17-1.12=2.05 at L/h=2) and reduces with higher L/h. The effect of transverse deformation is also observed to gain significance for shorter spans, albeit it is less influential than shear stresses. The PS/TB ratio is 1.12 at L/h=2 and reduces to 1.007 when L/h=14, suggesting it is negligible for long span beams.

Figure 8 Effect of the shear deformation on the prediction of the peak deflection

5.3. Example 3. Effect of support height

In the present formulation, origin O in Figure 1 does not necessarily need to coincide with the cross-sectional centroid. This feature is used in the present example to model supports that are offset from the centroid. In Example 2, the end supports were located at the section mid-height by locating origin O at the mid-height. We deviate from this convention in the present example, where origin O is moved to the bottom face of the beam (Figure 9). Figures 1.a-b provide a comparison of the longitudinal normal stress distribution at the top and bottom fibers against the longitudinal coordinate for a span L=3h. Unlike the Timoshenko beam theory whereby the longitudinal stresses at the extreme fibers have a parabolic distribution along the span, those predicted by the 3D FEA solution exhibit a more complex shape. In comparison to the 3D FEA, the present solution with n=3 underestimates the stress distributions along both top and bottom faces. As the number of terms n increases to 5 and 7, the stress distributions along the top fiber predicted by the present solution approach that of the of the 3D FEA solution (Figure 10.a). More terms are found necessary to attain convergence for the stresses on the bottom (Figure 10.b), where convergence is attained for n=9 in excellent agreement with the 3D FEA predictions and no further change is observed for n=10. Similar findings are observed for L=10h (Figures 10.c-d), where the solution with n=9 is observed to successfully capture the stress localization near the bottom supports. The longitudinal stress distribution for the case of mid-height support (as obtained from Example 2) based on the present solution with n=9 is overlaid on (Figures 10.a-d). Stress distributions at the top fibers for mid-height and bottom supports are comparable for the short-span beam (Figure 10.a), and nearly identical for the long-span beam, but considerable difference is observed between the stress distributions at bottom fiber between the bottom and mid-height support cases (Figures 10.b,d).

Figures 11.a-b depicts the stress profiles at the mid-span cross-section predicted for L=3h and L=10h, respectively. For the short span L=3h, the linear stress profile predicted by the present solution with n=3 is in close agreement with the Euler-Bernoulli and Timoshenko beam solutions, but slightly differs from the slightly nonlinear stress profile predicted by the present study with n=5, which is observed to nearly coincide with the 3D FEA. It of interest to note that the neutral axis in the latter two solutions is slightly shifted downwards from the section mid-height since the high transverse stresses provided by the end supports at the bottom slightly enlarge the section width based on the Poisson's ratio effect, which causes a downward shift of the deformed section centroid. This phenomenon has not been observed in Example 2 where the end supports were located at mid-height. For L/h=10 (Figure 11.b) the solutions based the present theory, the FEA, the Euler-Bernoulli beam, and the Timoshenko beam are in very close agreement. For the longer L/h ratio, the downward shift of the neutral axis becomes negligible since the width enlargement is localized at the supports and is far from mid-span.

Figure 12 depicts the transverse normal stress profiles at sections z=0.1L-0.5L as obtained from the present solution with n=9 for a span L=3h. Overlaid on the figure is the stress profile at z=0.1L as obtained from the 3D FEA. Close agreement is observed between the present solution and 3D FEA predictions. Unlike the case of mid-height support

in Example 2, stresses near the bottom face are significant. The stress profiles at sections from z=0.3L-0.5L are found almost identical. However, the stresses significantly increase as one approaches the support location.

Figure 9 Beams simply supported at the bottom fibers

Figure 10 Longitudinal normal stresses for (a) At top fiber L=3h (b) At bottom fiber L-3h, (c) at top fiber L=10h, and b) at bottom fiber L=10h

Figure 11 Longitudinal stress profiles at mid-span cross-section for spans (a) L=3h, (b) L=10h

Figure 12 Transverse normal stress profiles at sections z=0.1L, 0.2L, 0.3L, and 0.5L

5.4. Example 4. Longitudinal stress profiles in deep beams:

Carrera and Guita (2010) and Patel et al. (2014) showed that the nonlinear distribution of the longitudinal normal stress across the section depth is significant for beams with very short spans (e.g., $L/h = 2$). As observed in Example 3, the longitudinal normal stress profile at mid-span is slightly nonlinear for the span-to-depth ratio $L=3h$. The present solution is thus conducted to investigate the nonlinear stress profiles for the beam given in Example 3 with span-to-depth ratio L/h=1 and 2 and subjected to a downward traction $\sigma_y = 10MPa$ on the top face. Figures 13.a-b depict the stress profiles at the mid-span section obtained from the present solution with n=4, 5, 7, 8 and 9 for L/h=1 and 2, respectively. When $n = 3$ (not shown on the figure for clarity), the present solution coincides with Euler-Bernoulli profile and as n increases, the predicted profiles become highly nonlinear and convergence is attained when $n = 8$. Further increase of n is shown not to influence the predicted stress profile. The converged stress profiles are clearly nonlinear across the depth.

Figure 13 Longitudinal stress profiles at mid-span for spans (a) L=h and (b) L=2h

5.5. Example 5. Peak deflection of a cantilever beam with a monosymmetric cross-section

A cantilever steel beam with a WT250x200 cross-section (flange width 200mm, flange thickness 16mm, section depth 250mm and a web thickness 10mm) is subjected to a tip point load P=23.4 kN acting at the section centroid. The span-to-depth ratio is taken as 4. Young Modulus is taken as 200 GPa and Poisson's ratio is 0.3. The peak deflection predicted by the 3D FEA solution is 1.33 mm and is taken as a reference solution for comparison. The peak deflection predicted by the Euler-Bernoulli beam theory is 1.21mm, which is 9.0% less than that based on the 3D FEA. The present study with n=3 4 or 5 predicts a deflection 1.33mm which essentially coincides with the 3D FEA prediction. The example demonstrates the applicability of the present theory to monosymmetric sections.

6. Summary and Conclusions

The main contributions of the study are summarized in the following:

(1) A high-order beam theory was developed for the static analysis of beams. The longitudinal normal stress field was assumed as a series of power functions in the transverse coordinate $y^{i-1}\left(i=1,2...,n\right)$ multiplied by unknown functions $F_i\left(z\right)$ of the longitudinal coordinate z . The corresponding shear and transverse normal stress fields were then derived from the infinitesimal 2D equilibrium conditions and the traction boundary conditions were satisfied in an infinitesimal exact sense. The resulting stress fields were used in conjunction with the principle of stationary complementary strain energy to express the compatibility conditions in terms of the unknown functions $F_i\left(z\right)$ and derive the possible essential and natural boundary conditions. The differential equations of compatibility were found to be coupled and a general solution was developed for the system.

(2) Novel features of the theory include capturing the transverse normal stresses, in addition to longitudinal and shear stresses, material orthotropy, and nonlinear stress profiles. Unlike conventional solutions based on kinematic assumptions, which satisfy compatibility in an exact sense, but satisfy equilibrium conditions in an approximate integral sense, the present solution is based on postulated stress fields, and satisfies the 2D equilibrium condition in an exact sense, but satisfies the compatibility conditions in an average integral sense.

(3) The theory is applicable to flexural beam problems involving isotropic and orthotropic materials, doubly symmetric and monosymmetric cross-sections, as demonstrated through comparisons with classical beam and FEA solutions. Compared to conventional theories, the present theory was shown to offer modelling advantages in applications involving deep beams and/or with supports that are offset from the section centroid.

(4) Unlike conventional beam theories (e.g., Euler-Bernoulli, Timoshenko, etc.), the present solution avoids postulating any kinematic assumptions. As a result, the solution was shown to consistently converge to the displacements from above, in the sense that lower order stress polynomial solutions (i.e., small n) tend to overestimate the predicted deformations (i.e., underestimate the stiffness). As the polynomial order increases, the predicted displacements tend to reduce and approach those based on the 3D FEA in all cases examined.

(5) The assumed stress fields satisfy the traction boundary conditions at the top and bottom faces of the beam in an exact sense, a feature that is un-attainable under displacement-based 3D FEA solutions (e.g., Example 2) where the traction boundary conditions were shown to be satisfied only approximately.

(6) Within the family of solutions developed, when the number of stress terms is $n=3$, the resulting longitudinal normal stress has a linear solution and the present theory provides results that are close, but not identical, to the Timoshenko beam theory predictions. The slight difference observed is attributed to the fact that the present theory captures the transverse stresses which are omitted in the Timoshenko beam theory. When the number of stress terms is $n \geq 4$, the present theory is able to capture the nonlinear stress profiles that may arise in deep beams and/or beams with supports that are offset from the section centroid. The number of stress terms required to attain convergence depends on the beam span to depth ratio.

(7) The examples investigated showed that stress distribution near the end support highly depend on the support location relative to the section centroid. While supports at the centroid were associated with little nonlinearity of the stress profiles, bottom supports were associated with highly nonlinear stress distributions as predicted by the present solution and the 3D FEA.

(8) For the case of bottom supports, the present theory and the 3D FEA predict significant transverse normal stresses near the supports.

Appendix 1: Definition of terms appearing the stress expressions

This appendix provides the steps for characterizing the terms appearing in Eqs. (3) and (8).

(1) Define the functions:

$$\alpha_i(y)=\left[1/b(y)\right]\int_{-h_1}^{y} b(\xi)\xi^{i-1}d\xi; \qquad \beta_i(y)=\left[1/b(y)\right]\int_{-h_1}^{y}\int_{-h_1}^{\eta} b(\xi)\xi^{i-1}d\xi d\eta \tag{53a-b}$$

where i ranges from 1 to $m=n-2$.

(2) Determine the generated tractions:

$$\bar{\tau}(y,z)=\left[1/b(y)\right]\left\{b(-h_1)\tau(-h_1,z)+\int_{-h_1}^{y}b(\xi)\,p_z(\xi,z)\,d\xi\right\}$$

$$\bar{\sigma}_y(y,z)=\left[1/b(y)\right]\left\{b(-h_1)\sigma_y(-h_1,z)+\int_{-h_1}^{y}b(\xi)\,p_y(\xi,z)\,d\xi\right.$$
$$\left.-b(-h_1)\partial\left[\tau(-h_1,z)\right]/\partial z-\int_{-h_1}^{y}\int_{-h_1}^{\eta}b(\xi)\left[\partial p_z(\xi,z)/\partial z\right]d\xi d\eta\right\} \tag{54}$$

(3) Given $\alpha_i(y)$ as defined in Eq. (53a), determine the constants:

$$\bar{\alpha}_i=\int_{A_{0w}}y^i dA,\quad \hat{\alpha}_i=\int_{A_{0\tau}}\alpha_i(y)\,dA \tag{55}$$

where A_{0w} and $A_{0\tau}$ are area parts of member cross-section at $z=0$ where prescribed longitudinal and transverse displacements, respectively are applied as boundary conditions.

(4) Given $\alpha_i(y)$ in Eq. (44a), $\bar{\alpha}_i$ and $\hat{\alpha}_i$ in Eqs. (55) and the applied tractions in Eqs. (45), determine:

$$\varsigma_{11}=-\frac{\alpha_n(h_2)\int_A\bar{\tau}(y,0)\,dA-\hat{\alpha}_n\left[\bar{\tau}(h_2,0)-\tau(h_2,0)\right]}{\hat{\alpha}_n\alpha_{n-1}(h_2)-\hat{\alpha}_{n-1}\alpha_n(h_2)};\qquad \varsigma_{12}=\frac{\alpha_n(h_2)}{\hat{\alpha}_n\alpha_{n-1}(h_2)-\hat{\alpha}_{n-1}\alpha_n(h_2)};$$

$$\varsigma_{21}=\frac{\alpha_{n-1}(h_2)\int_A\bar{\tau}(y,0)\,dA-\hat{\alpha}_{n-1}\left[\bar{\tau}(h_2,0)-\tau(h_2,0)\right]}{\hat{\alpha}_n\alpha_{n-1}(h_2)-\hat{\alpha}_{n-1}\alpha_n(h_2)};\quad \varsigma_{22}=-\frac{\alpha_{n-1}(h_2)}{\hat{\alpha}_n\alpha_{n-1}(h_2)-\hat{\alpha}_{n-1}\alpha_n(h_2)};$$

$$\varsigma_{31}=\frac{\bar{\alpha}_n}{\bar{\alpha}_n\bar{\alpha}_{n-2}-\bar{\alpha}_{n-1}\bar{\alpha}_{n-1}};\qquad \varsigma_{32}=-\frac{\bar{\alpha}_{n-1}}{\bar{\alpha}_n\bar{\alpha}_{n-2}-\bar{\alpha}_{n-1}\bar{\alpha}_{n-1}};$$

$$\varsigma_{41}=-\frac{\bar{\alpha}_{n-1}}{\bar{\alpha}_n\bar{\alpha}_{n-2}-\bar{\alpha}_{n-1}\bar{\alpha}_{n-1}};\qquad \varsigma_{42}=\frac{\bar{\alpha}_{n-2}}{\bar{\alpha}_n\bar{\alpha}_{n-2}-\bar{\alpha}_{n-1}\bar{\alpha}_{n-1}};$$

$$\varsigma_{13i}=\frac{\alpha_n(h_2)\hat{\alpha}_i-\hat{\alpha}_n\alpha_i(h_2)}{\hat{\alpha}_n\alpha_{n-1}(h_2)-\hat{\alpha}_{n-1}\alpha_n(h_2)};\qquad \varsigma_{23i}=-\frac{\alpha_{n-1}(h_2)\hat{\alpha}_i-\hat{\alpha}_{n-1}\alpha_i(h_2)}{\hat{\alpha}_n\alpha_{n-1}(h_2)-\hat{\alpha}_{n-1}\alpha_n(h_2)};$$

$$\varsigma_{33i}=-\frac{\bar{\alpha}_n\bar{\alpha}_{i-1}-\bar{\alpha}_{n-1}\bar{\alpha}_i}{\bar{\alpha}_n\bar{\alpha}_{n-2}-\bar{\alpha}_{n-1}\bar{\alpha}_{n-1}};\qquad \varsigma_{43i}=\frac{\bar{\alpha}_{n-1}\bar{\alpha}_{i-1}-\bar{\alpha}_{n-2}\bar{\alpha}_i}{\bar{\alpha}_n\bar{\alpha}_{n-2}-\bar{\alpha}_{n-1}\bar{\alpha}_{n-1}}; \tag{56}$$

(5) Starting from the definitions of $\alpha_i(y),\beta_i(y)$ as provided in Eqs. Eq. (53a-b), determine the following constants

$$\lambda_{1i}=\frac{\alpha_n(h_2)\beta_i(h_2)-\beta_n(h_2)\alpha_i(h_2)}{\alpha_n(h_2)\beta_{n-1}(h_2)-\alpha_{n-1}(h_2)\beta_n(h_2)};\quad \lambda_{2i}=-\frac{\alpha_{n-1}(h_2)\beta_i(h_2)-\beta_{n-1}(h_2)\alpha_i(h_2)}{\alpha_n(h_2)\beta_{n-1}(h_2)-\alpha_{n-1}(h_2)\beta_n(h_2)}; \tag{57}$$

(6) Also, starting from the definitions of $\alpha_i(y),\beta_i(y)$ as provided in Eqs. (44a,b) and the applied traction (i.e., $\sigma_y(h_1,z)$, $\tau(h_1,z)$, $\sigma_y(h_2,z)$, $\tau(h_2,z)$), determine the following constants

$$\rho_1(z)=\frac{\alpha_n(h_2)\left[\sigma_y(h_2,z)-\bar{\sigma}_y(h_2,z)\right]-\beta_n(h_2)\left[\bar{\tau}'(h_2,z)-\tau'(h_2,z)\right]}{\alpha_n(h_2)\beta_{n-1}(h_2)-\alpha_{n-1}(h_2)\beta_n(h_2)},$$

$$\rho_2(z)=-\frac{\alpha_{n-1}(h_2)\left[\sigma_y(h_2,z)-\bar{\sigma}_y(h_2,z)\right]-\beta_{n-1}(h_2)\left[\bar{\tau}'(h_2,z)-\tau'(h_2,z)\right]}{\alpha_n(h_2)\beta_{n-1}(h_2)-\alpha_{n-1}(h_2)\beta_n(h_2)} \tag{58}$$

(7) Given ς_{ij} as obtained in Eq. (56), $\lambda_{1i}, \lambda_{2i}$ as given in Eq. (57) and $\alpha_i(y)$ in Eqs. (44a), the following distribution functions of the $y-$ coordinated are defined:

$$
\begin{aligned}
&\eta_{12}(y) = y^{n-2}\varsigma_{31} + y^{n-1}\varsigma_{41}; \qquad \eta_{13}(y) = y^{n-2}\varsigma_{12} + y^{n-1}\varsigma_{22};\\
&\eta_{14}(y) = y^{n-2}\varsigma_{32} + y^{n-1}\varsigma_{42}; \qquad \eta_{22}(y) = -\left[\alpha_{n-1}(y)\varsigma_{12} + \alpha_n(y)\varsigma_{22}\right];\\
&\xi_{1i}(y) = y^{i-1} - y^{n-2}\lambda_{1i} - y^{n-1}\lambda_{2i}; \quad \xi_{2i}(y) = \alpha_{n-1}(y)\lambda_{1i} + \alpha_n(y)\lambda_{2i} - \alpha_i(y);\\
&\xi_{3i}(y) = \beta_i(y) - \beta_{n-1}(y)\lambda_{1i} - \beta_n(y)\lambda_{2i};\\
&\psi_{1i}(y) = y^{n-2}\varsigma_{13i} + y^{n-1}\varsigma_{23i} + y^{n-2}\lambda_{1i} + y^{n-1}\lambda_{2i};\\
&\psi_{2i}(y) = y^{n-2}\varsigma_{33i} + y^{n-1}\varsigma_{43i} + y^{n-2}\lambda_{1i} + y^{n-1}\lambda_{2i};\\
&\psi_{3i}(y) = -\alpha_{n-1}(y)\varsigma_{13i} - \alpha_n(y)\varsigma_{23i} - \alpha_{n-1}(y)\lambda_{1i} - \alpha_n(y)\lambda_{2i}; \qquad i = 1,\ldots,m
\end{aligned}
\tag{59}
$$

(8) Given functions $\psi_{1i}(y)$, $\psi_{2i}(y)$ and $\psi_{3i}(y)$ from Eqs. (59), the following vector functions of the $y-$ coordinates are defined:

$$
\begin{aligned}
&\boldsymbol{\psi}_1(y)^{\mathbf{T}}_{1\times m} = \left\langle \psi_{11}(y) \quad \ldots \quad \psi_{1i}(y) \quad \ldots \quad \psi_{1m}(y) \right\rangle;\\
&\boldsymbol{\psi}_2(y)^{\mathbf{T}}_{1\times m} = \left\langle \psi_{21}(y) \quad \ldots \quad \psi_{2i}(y) \quad \ldots \quad \psi_{2m}(y) \right\rangle;\\
&\boldsymbol{\psi}_3(y)^{\mathbf{T}}_{1\times m} = \left\langle \psi_{31}(y) \quad \ldots \quad \psi_{3i}(y) \quad \ldots \quad \psi_{3m}(y) \right\rangle;
\end{aligned}
\tag{60}
$$

(9) Given Eqs. (59) and (60), determine the following vectors

$$
\begin{aligned}
&\hat{\boldsymbol{\chi}}(y)^{\mathbf{T}}_{1\times 3(m+1)} = \left\langle \boldsymbol{\xi}_1(y)^{\mathbf{T}}_{1\times m} \;\vdots\; \boldsymbol{\psi}_2(y)^{\mathbf{T}}_{1\times m} \quad \boldsymbol{\psi}_1(y)^{\mathbf{T}}_{1\times m} \;\vdots\; \eta_{12}(y) \quad \eta_{13}(y) \quad \eta_{14}(y) \right\rangle\\
&\tilde{\boldsymbol{\chi}}(y)^{\mathbf{T}}_{1\times(2m+1)} = \left\langle \boldsymbol{\xi}_2(y)^{\mathbf{T}}_{1\times m} \;\vdots\; \boldsymbol{\psi}_3(y)^{\mathbf{T}}_{1\times m} \;\vdots\; \eta_{22}(y) \right\rangle\\
&\boldsymbol{\xi}_1(y)^{\mathbf{T}}_{1\times m} = \left\langle \xi_{11}(y) \quad \ldots \quad \xi_{1i}(y) \quad \ldots \quad \xi_{1m}(y) \right\rangle\\
&\boldsymbol{\xi}_2(y)^{\mathbf{T}}_{1\times m} = \left\langle \xi_{21}(y) \quad \ldots \quad \xi_{2i}(y) \quad \ldots \quad \xi_{2m}(y) \right\rangle\\
&\boldsymbol{\xi}_3(y)^{\mathbf{T}}_{1\times m} = \left\langle \xi_{31}(y) \quad \ldots \quad \xi_{3i}(y) \quad \ldots \quad \xi_{3m}(y) \right\rangle
\end{aligned}
\tag{61}
$$

(10) Given the terms $\rho_1(z)$, $\rho_2(z)$ defined in Eqs. (58), ς_{11} and ς_{21} in Eq. (56), $\bar{\tau}(y,z)$, $\bar{\sigma}_y(y,z)$ in Eq. (54), and the vectors defined in Eq. (61), one can determine the stress field expressions $\sigma_z^*(y,z), \tau^*(y,z).\sigma_y^*(y,z)$ appearing in Eq. (5).

Appendix 2: Vectors and Matrices appearing in boundary equations

The boundary conditions Eqs. (39)-(45) were expressed in terms of matrices $\mathbf{b_{ij}}$ defined as

$$
\begin{aligned}
\left[\mathbf{b_{11}}\right]_{m\times 4m} = &\int_0^L \left\{ \hat{\mathbf{I}}_2\mathbf{C_{11}}\hat{\mathbf{I}}_1^{\mathbf{T}}\left[\mathbf{H_1}(z)\right]_{m\times 4m} - \hat{\mathbf{I}}_2\mathbf{C_{12}}\left[\mathbf{H_1}''(z)\right]_{m\times 4m} + \hat{\mathbf{I}}_2\mathbf{C_{11}}\hat{\mathbf{I}}_2^{\mathbf{T}}\left[\mathbf{H_1}(0)\right]_{m\times 4m} \right\} + \mathbf{C_{22}}\left[\mathbf{H_1}'''(0)\right]_{m\times 4m}\\
&+\left(\int_0^L \hat{\mathbf{I}}_2\mathbf{C_{11}}\hat{\mathbf{I}}_3^{\mathbf{T}} z dz - \mathbf{C_{12}^T}\hat{\mathbf{I}}_1^{\mathbf{T}} - \mathbf{C_{12}^T}\hat{\mathbf{I}}_3^{\mathbf{T}} - \tilde{\mathbf{I}}_1\mathbf{C_{33}}\tilde{\mathbf{I}}_1^{\mathbf{T}} - \tilde{\mathbf{I}}_1\mathbf{C_{33}}\tilde{\mathbf{I}}_2^{\mathbf{T}} \right)\left[\mathbf{H_1}'(0)\right]_{m\times 4m},
\end{aligned}
$$

$$\{\mathbf{b}_{12}\}_{m\times 1}=\int_0^L\left(\hat{\mathbf{I}}_2\mathbf{C}_{11}\hat{\mathbf{I}}_1^{\mathrm{T}}\{\mathbf{H}_2\}_{m\times 1}+\hat{\mathbf{I}}_2\mathbf{C}_{11}\hat{\mathbf{I}}_2^{\mathrm{T}}\{\mathbf{H}_2\}_{m\times 1}+\hat{\mathbf{I}}_2\mathbf{C}_{11}\hat{\mathbf{I}}_4^{\mathrm{T}}\right)dz,$$

530
$$\{\mathbf{b}_{13}\}_{m\times 1}=\int_0^L\hat{\mathbf{I}}_2\mathbf{C}_{11}\hat{\mathbf{I}}_1^{\mathrm{T}}z\{\mathbf{H}_3\}_{m\times 1}dz+\left(\int_0^L z\hat{\mathbf{I}}_2\mathbf{C}_{11}\hat{\mathbf{I}}_3^{\mathrm{T}}dz-\mathbf{C}_{12}^{\mathrm{T}}\hat{\mathbf{I}}_1^{\mathrm{T}}-\mathbf{C}_{12}^{\mathrm{T}}\hat{\mathbf{I}}_3^{\mathrm{T}}-\tilde{\mathbf{I}}_1\mathbf{C}_{33}\tilde{\mathbf{I}}_1^{\mathrm{T}}-\tilde{\mathbf{I}}_1\mathbf{C}_{33}\tilde{\mathbf{I}}_2^{\mathrm{T}}\right)\{\mathbf{H}_3\}_{m\times 1}+$$
$$+\left(\int_0^L z\hat{\mathbf{I}}_2\mathbf{C}_{11}\hat{\mathbf{I}}_5^{\mathrm{T}}dz-\mathbf{C}_{12}^{\mathrm{T}}\hat{\mathbf{I}}_5^{\mathrm{T}}-\tilde{\mathbf{I}}_1\mathbf{C}_{33}\tilde{\mathbf{I}}_3^{\mathrm{T}}\right),$$

$$\{\mathbf{b}_{14}\}_{m\times 1}=\int_0^L\hat{\mathbf{I}}_2\mathbf{C}_{11}\hat{\mathbf{I}}_1^{\mathrm{T}}\{\mathbf{H}_4\}_{m\times 1}dz+\int_0^L\hat{\mathbf{I}}_2\mathbf{C}_{11}\hat{\mathbf{I}}_2^{\mathrm{T}}\{\mathbf{H}_4\}_{m\times 1}dz+\int_0^L\hat{\mathbf{I}}_2\mathbf{C}_{11}\hat{\mathbf{I}}_6^{\mathrm{T}}dz,$$

$$[\mathbf{b}_{21}]_{m\times 4m}=\int_0^L\left(z\hat{\mathbf{I}}_3\mathbf{C}_{11}\hat{\mathbf{I}}_1^{\mathrm{T}}[\mathbf{H}_1(z)]_{m\times 4m}+\tilde{\mathbf{I}}_2\mathbf{C}_{33}\tilde{\mathbf{I}}_1^{\mathrm{T}}[\mathbf{H}_1'(z)]_{m\times 4m}-z\hat{\mathbf{I}}_3\mathbf{C}_{12}[\mathbf{H}_1''(z)]_{m\times 4m}\right)dz$$

531
$$-\mathbf{C}_{22}[\mathbf{H}_1''(0)]_{m\times 4m}+\left(\int_0^L z\hat{\mathbf{I}}_3\mathbf{C}_{11}\hat{\mathbf{I}}_2^{\mathrm{T}}dz+\mathbf{C}_{12}^{\mathrm{T}}\hat{\mathbf{I}}_1^{\mathrm{T}}+\mathbf{C}_{12}^{\mathrm{T}}\hat{\mathbf{I}}_2^{\mathrm{T}}\right)[\mathbf{H}_1(0)]_{m\times 4m}+$$
$$+\left(\int_0^L z^2\hat{\mathbf{I}}_3\mathbf{C}_{11}\hat{\mathbf{I}}_3^{\mathrm{T}}dz+\int_0^L\tilde{\mathbf{I}}_2\mathbf{C}_{33}\tilde{\mathbf{I}}_2^{\mathrm{T}}dz\right)[\mathbf{H}_1'(0)]_{m\times 4m},$$

$$\{\mathbf{b}_{22}\}_{m\times 1}=\int_0^L z\hat{\mathbf{I}}_3\mathbf{C}_{11}\hat{\mathbf{I}}_1^{\mathrm{T}}\{\mathbf{H}_2\}_{m\times 1}dz+\left(\int_0^L z\hat{\mathbf{I}}_3\mathbf{C}_{11}\hat{\mathbf{I}}_2^{\mathrm{T}}dz+\mathbf{C}_{12}^{\mathrm{T}}\hat{\mathbf{I}}_1^{\mathrm{T}}+\mathbf{C}_{12}^{\mathrm{T}}\hat{\mathbf{I}}_2^{\mathrm{T}}\right)\{\mathbf{H}_2\}_{m\times 1}+\int_0^L z\hat{\mathbf{I}}_3\mathbf{C}_{11}\hat{\mathbf{I}}_4^{\mathrm{T}}dz+\mathbf{C}_{12}^{\mathrm{T}}\hat{\mathbf{I}}_4^{\mathrm{T}},$$

$$\{\mathbf{b}_{23}\}_{m\times 1}=\int_0^L\left\{\left[z\hat{\mathbf{I}}_3\mathbf{C}_{11}\hat{\mathbf{I}}_1^{\mathrm{T}}z+\tilde{\mathbf{I}}_2\mathbf{C}_{33}\tilde{\mathbf{I}}_1^{\mathrm{T}}+z^2\hat{\mathbf{I}}_3\mathbf{C}_{11}\hat{\mathbf{I}}_3^{\mathrm{T}}+\tilde{\mathbf{I}}_2\mathbf{C}_{33}\tilde{\mathbf{I}}_2^{\mathrm{T}}dz\right]\{\mathbf{H}_3\}_{m\times 1}+z^2\hat{\mathbf{I}}_3\mathbf{C}_{11}\hat{\mathbf{I}}_5^{\mathrm{T}}+\tilde{\mathbf{I}}_2\mathbf{C}_{33}\tilde{\mathbf{I}}_3^{\mathrm{T}}\right\}dz,$$

532
$$\{\mathbf{b}_{24}\}_{m\times 1}=\int_0^L z\left(\hat{\mathbf{I}}_3\mathbf{C}_{11}\hat{\mathbf{I}}_1^{\mathrm{T}}\{\mathbf{H}_4\}_{m\times 1}+\hat{\mathbf{I}}_3\mathbf{C}_{11}\hat{\mathbf{I}}_6^{\mathrm{T}}\right)dz+\left(\int_0^L z\hat{\mathbf{I}}_3\mathbf{C}_{11}\hat{\mathbf{I}}_2^{\mathrm{T}}dz+\mathbf{C}_{12}^{\mathrm{T}}\hat{\mathbf{I}}_1^{\mathrm{T}}+\mathbf{C}_{12}^{\mathrm{T}}\hat{\mathbf{I}}_2^{\mathrm{T}}\right)\{\mathbf{H}_4\}_{m\times 1}+\mathbf{C}_{12}^{\mathrm{T}}\hat{\mathbf{I}}_6^{\mathrm{T}},$$

$$[\mathbf{b}_{31}]_{m\times 4m}=\left(-\mathbf{C}_{12}^{\mathrm{T}}\hat{\mathbf{I}}_1^{\mathrm{T}}-\tilde{\mathbf{I}}_1\mathbf{C}_{33}\tilde{\mathbf{I}}_1^{\mathrm{T}}\right)[\mathbf{H}_1'(L)]_{m\times 4m}+\mathbf{C}_{22}[\mathbf{H}_1'''(L)]_{m\times 4m}+\left(-\mathbf{C}_{12}^{\mathrm{T}}\hat{\mathbf{I}}_3^{\mathrm{T}}-\tilde{\mathbf{I}}_1\mathbf{C}_{33}\tilde{\mathbf{I}}_2^{\mathrm{T}}\right)[\mathbf{H}_1'(0)]_{m\times 4m},$$

$$\{\mathbf{b}_{32}\}_{m\times 1}=\left(-\mathbf{C}_{12}^{\mathrm{T}}\hat{\mathbf{I}}_1^{\mathrm{T}}-\tilde{\mathbf{I}}_1\mathbf{C}_{33}\tilde{\mathbf{I}}_1^{\mathrm{T}}\right)\{\mathbf{H}_3\}_{m\times 1}+\left(-\mathbf{C}_{12}^{\mathrm{T}}\hat{\mathbf{I}}_3^{\mathrm{T}}-\tilde{\mathbf{I}}_1\mathbf{C}_{33}\tilde{\mathbf{I}}_2^{\mathrm{T}}\right)\{\mathbf{H}_3\}_{m\times 1}-\mathbf{C}_{12}^{\mathrm{T}}\hat{\mathbf{I}}_5^{\mathrm{T}}-\tilde{\mathbf{I}}_1\mathbf{C}_{33}\tilde{\mathbf{I}}_3^{\mathrm{T}},$$

$$[\mathbf{b}_{41}]_{m\times 4m}=-\mathbf{C}_{12}^{\mathrm{T}}\hat{\mathbf{I}}_1^{\mathrm{T}}[\mathbf{H}_1(L)]_{m\times 4m}+\mathbf{C}_{22}[\mathbf{H}_1''(L)]_{m\times 4m}-L\mathbf{C}_{12}^{\mathrm{T}}\hat{\mathbf{I}}_3^{\mathrm{T}}[\mathbf{H}_1'(0)]_{m\times 4m}-\mathbf{C}_{12}^{\mathrm{T}}\hat{\mathbf{I}}_2^{\mathrm{T}}[\mathbf{H}_1(0)]_{m\times 4m},$$

$$\{\mathbf{b}_{42}\}_{m\times 1}=-\mathbf{C}_{12}^{\mathrm{T}}\hat{\mathbf{I}}_1^{\mathrm{T}}\{\mathbf{H}_2\}_{m\times 1}-\mathbf{C}_{12}^{\mathrm{T}}\hat{\mathbf{I}}_2^{\mathrm{T}}\{\mathbf{H}_2\}_{m\times 1}-\mathbf{C}_{12}^{\mathrm{T}}\hat{\mathbf{I}}_4^{\mathrm{T}},$$

533
$$\{\mathbf{b}_{43}\}_{m\times 1}=-\mathbf{C}_{12}^{\mathrm{T}}\hat{\mathbf{I}}_1^{\mathrm{T}}L\{\mathbf{H}_3\}_{m\times 1}-L\mathbf{C}_{12}^{\mathrm{T}}\hat{\mathbf{I}}_3^{\mathrm{T}}\{\mathbf{H}_3\}_{m\times 1}-L\mathbf{C}_{12}^{\mathrm{T}}\hat{\mathbf{I}}_5^{\mathrm{T}},$$

$$\{\mathbf{b}_{44}\}_{m\times 1}=-\mathbf{C}_{12}^{\mathrm{T}}\hat{\mathbf{I}}_1^{\mathrm{T}}\{\mathbf{H}_4\}_{m\times 1}-\mathbf{C}_{12}^{\mathrm{T}}\hat{\mathbf{I}}_2^{\mathrm{T}}\{\mathbf{H}_4\}_{m\times 1}-\mathbf{C}_{12}^{\mathrm{T}}\hat{\mathbf{I}}_6^{\mathrm{T}},$$

$$[\mathbf{b}_{51}]_{m\times 4m}=\int_0^L\left(\hat{\mathbf{I}}_4\mathbf{C}_{11}\hat{\mathbf{I}}_1^{\mathrm{T}}[\mathbf{H}_1(z)]_{m\times 4m}-\hat{\mathbf{I}}_4\mathbf{C}_{12}[\mathbf{H}_1''(z)]_{m\times 4m}+\hat{\mathbf{I}}_4\mathbf{C}_{11}\hat{\mathbf{I}}_2^{\mathrm{T}}[\mathbf{H}_1(0)]_{m\times 4m}+\hat{\mathbf{I}}_4\mathbf{C}_{11}\hat{\mathbf{I}}_3^{\mathrm{T}}z[\mathbf{H}_1'(0)]_{m\times 4m}\right)dz,$$

$$\{\mathbf{b}_{52}\}_{m\times 1}=\int_0^L\left(\hat{\mathbf{I}}_4\mathbf{C}_{11}\hat{\mathbf{I}}_1^{\mathrm{T}}\{\mathbf{H}_2\}_{m\times 1}+\hat{\mathbf{I}}_4\mathbf{C}_{11}\hat{\mathbf{I}}_2^{\mathrm{T}}\{\mathbf{H}_2\}_{m\times 1}+\hat{\mathbf{I}}_4\mathbf{C}_{11}\hat{\mathbf{I}}_4^{\mathrm{T}}\right)dz,$$

$$\{\mathbf{b}_{53}\}_{m\times 1}=\int_0^L\left(\hat{\mathbf{I}}_4\mathbf{C}_{11}\hat{\mathbf{I}}_1^{\mathrm{T}}z\{\mathbf{H}_3\}_{m\times 1}+\hat{\mathbf{I}}_4\mathbf{C}_{11}\hat{\mathbf{I}}_3^{\mathrm{T}}z\{\mathbf{H}_3\}_{m\times 1}+\hat{\mathbf{I}}_4\mathbf{C}_{11}\hat{\mathbf{I}}_5^{\mathrm{T}}z\right)dz,$$

$$\{\mathbf{b}_{54}\}_{m\times 1}=\int_0^L\left(\hat{\mathbf{I}}_4\mathbf{C}_{11}\hat{\mathbf{I}}_1^{\mathrm{T}}\{\mathbf{H}_4\}_{m\times 1}+\hat{\mathbf{I}}_4\mathbf{C}_{11}\hat{\mathbf{I}}_2^{\mathrm{T}}\{\mathbf{H}_4\}_{m\times 1}+\hat{\mathbf{I}}_4\mathbf{C}_{11}\hat{\mathbf{I}}_6^{\mathrm{T}}\right)dz,$$

534
$$[\mathbf{b}_{61}]_{m\times 4m}=\int_0^L\left(z\hat{\mathbf{I}}_5\mathbf{C}_{11}\hat{\mathbf{I}}_1^{\mathrm{T}}[\mathbf{H}_1(z)]_{m\times 4m}+\tilde{\mathbf{I}}_3\mathbf{C}_{33}\tilde{\mathbf{I}}_1^{\mathrm{T}}[\mathbf{H}_1'(z)]_{m\times 4m}-z\hat{\mathbf{I}}_5\mathbf{C}_{12}[\mathbf{H}_1''(z)]_{m\times 4m}+\right.$$
$$\left.+z\hat{\mathbf{I}}_5\mathbf{C}_{11}\hat{\mathbf{I}}_2^{\mathrm{T}}[\mathbf{H}_1(0)]_{m\times 4m}+\left(z^2\hat{\mathbf{I}}_5\mathbf{C}_{11}\hat{\mathbf{I}}_3^{\mathrm{T}}+\tilde{\mathbf{I}}_3\mathbf{C}_{33}\tilde{\mathbf{I}}_2^{\mathrm{T}}\right)[\mathbf{H}_1'(0)]_{m\times 4m}\right)dz,$$

$$\left\{\mathbf{b}_{62}\right\}_{m\times1}=\int_0^L\left(z\hat{\mathbf{I}}_5\mathbf{C}_{11}\hat{\mathbf{I}}_1^{\mathrm{T}}\left\{\mathbf{H}_2\right\}_{m\times1}+z\hat{\mathbf{I}}_5\mathbf{C}_{11}\hat{\mathbf{I}}_2^{\mathrm{T}}\left\{\mathbf{H}_2\right\}_{m\times1}+z\hat{\mathbf{I}}_5\mathbf{C}_{11}\hat{\mathbf{I}}_4^{\mathrm{T}}\right)dz,$$

$$\left\{\mathbf{b}_{63}\right\}_{m\times1}=\int_0^L\left(z\hat{\mathbf{I}}_5\mathbf{C}_{11}\hat{\mathbf{I}}_1^{\mathrm{T}}z\left\{\mathbf{H}_3\right\}_{m\times1}+\tilde{\mathbf{I}}_3\mathbf{C}_{33}\tilde{\mathbf{I}}_1^{\mathrm{T}}\left\{\mathbf{H}_3\right\}_{m\times1}+z^2\hat{\mathbf{I}}_5\mathbf{C}_{11}\hat{\mathbf{I}}_5^{\mathrm{T}}+\tilde{\mathbf{I}}_3\mathbf{C}_{33}\tilde{\mathbf{I}}_3^{\mathrm{T}}+\left(z^2\hat{\mathbf{I}}_5\mathbf{C}_{11}\hat{\mathbf{I}}_3^{\mathrm{T}}+\tilde{\mathbf{I}}_3\mathbf{C}_{33}\tilde{\mathbf{I}}_2^{\mathrm{T}}\right)\left\{\mathbf{H}_3\right\}_{m\times1}\right)dz,$$

$$\left\{\mathbf{b}_{64}\left(z\right)\right\}_{m\times1}=\int_0^L\left(z\hat{\mathbf{I}}_5\mathbf{C}_{11}\hat{\mathbf{I}}_1^{\mathrm{T}}\left\{\mathbf{H}_4\right\}_{m\times1}+z\hat{\mathbf{I}}_5\mathbf{C}_{11}\hat{\mathbf{I}}_2^{\mathrm{T}}\left\{\mathbf{H}_4\right\}_{m\times1}+z\hat{\mathbf{I}}_5\mathbf{C}_{11}\hat{\mathbf{I}}_6^{\mathrm{T}}\right)dz,$$

$$\left[\mathbf{b}_{71}\right]_{m\times4m}=\int_0^L\left\{\hat{\mathbf{I}}_6\mathbf{C}_{11}\hat{\mathbf{I}}_1^{\mathrm{T}}\left[\mathbf{H}_1\left(z\right)\right]_{m\times4m}-\hat{\mathbf{I}}_6\mathbf{C}_{12}\left[\mathbf{H}_1''\left(z\right)\right]_{m\times4m}+\hat{\mathbf{I}}_6\mathbf{C}_{11}\hat{\mathbf{I}}_2^{\mathrm{T}}\left[\mathbf{H}_1\left(0\right)\right]_{m\times4m}+z\hat{\mathbf{I}}_6\mathbf{C}_{11}\hat{\mathbf{I}}_3^{\mathrm{T}}\left[\mathbf{H}_1'\left(0\right)\right]_{m\times4m}\right\}dz,$$

$$\left\{\mathbf{b}_{72}\right\}_{m\times1}=\int_0^L\left(\hat{\mathbf{I}}_6\mathbf{C}_{11}\hat{\mathbf{I}}_1^{\mathrm{T}}\left\{\mathbf{H}_2\right\}_{m\times1}+\hat{\mathbf{I}}_6\mathbf{C}_{11}\hat{\mathbf{I}}_2^{\mathrm{T}}\left\{\mathbf{H}_2\right\}_{m\times1}+\hat{\mathbf{I}}_6\mathbf{C}_{11}\hat{\mathbf{I}}_4^{\mathrm{T}}\right)dz,$$

$$\left\{\mathbf{b}_{73}\right\}_{m\times1}=\int_0^L\left(\hat{\mathbf{I}}_6\mathbf{C}_{11}\hat{\mathbf{I}}_1^{\mathrm{T}}z\left\{\mathbf{H}_3\right\}_{m\times1}+z\hat{\mathbf{I}}_6\mathbf{C}_{11}\hat{\mathbf{I}}_3^{\mathrm{T}}\left\{\mathbf{H}_3\right\}_{m\times1}+z\hat{\mathbf{I}}_6\mathbf{C}_{11}\hat{\mathbf{I}}_5^{\mathrm{T}}\right)dz,$$

$$\left\{\mathbf{b}_{74}\right\}_{m\times1}=\int_0^L\left(\hat{\mathbf{I}}_6\mathbf{C}_{11}\hat{\mathbf{I}}_1^{\mathrm{T}}\left\{\mathbf{H}_4\right\}_{m\times1}+\hat{\mathbf{I}}_6\mathbf{C}_{11}\hat{\mathbf{I}}_2^{\mathrm{T}}\left\{\mathbf{H}_4\right\}_{m\times1}+\hat{\mathbf{I}}_6\mathbf{C}_{11}\hat{\mathbf{I}}_6^{\mathrm{T}}\right)dz.$$

Also, Eqs. (39)-(45) were expressed in terms of the following load vectors $\left\{\mathbf{L}_i\right\}_{m\times1}$

$$\left\{\mathbf{L}_1\right\}_{m\times1}=\int_0^L\left\{\hat{\mathbf{I}}_2\mathbf{C}_{11}\hat{\mathbf{I}}_1^{\mathrm{T}}\left\{\mathbf{H}_5\left(z\right)\right\}_{m\times1}-\hat{\mathbf{I}}_2\mathbf{C}_{12}\left\{\mathbf{H}_5''\left(z\right)\right\}_{m\times1}+\hat{\mathbf{I}}_2\mathbf{C}_{11}\hat{\mathbf{I}}_2^{\mathrm{T}}\left\{\mathbf{H}_5\left(0\right)\right\}_{m\times1}+\hat{\mathbf{I}}_2\mathbf{C}_{11}\hat{\mathbf{I}}_3^{\mathrm{T}}z+\hat{\mathbf{I}}_2\mathbf{d}_1\left(\mathbf{z}\right)\right\}dz$$

$$+\mathbf{C}_{22}\left\{\mathbf{H}_5'''\left(0\right)\right\}_{m\times1}-\left(\mathbf{C}_{12}^{\mathrm{T}}\hat{\mathbf{I}}_1^{\mathrm{T}}+\mathbf{C}_{12}^{\mathrm{T}}\hat{\mathbf{I}}_3^{\mathrm{T}}+\tilde{\mathbf{I}}_1\mathbf{C}_{33}\tilde{\mathbf{I}}_1^{\mathrm{T}}+\tilde{\mathbf{I}}_1\mathbf{C}_{33}\tilde{\mathbf{I}}_2^{\mathrm{T}}\right)\left\{\mathbf{H}_5'\left(0\right)\right\}_{m\times1}+\mathbf{d}_2'\left(0\right)+\tilde{\mathbf{I}}_1\mathbf{d}_3\left(0\right),$$

$$\left\{\mathbf{L}_2\right\}_{m\times1}=\int_0^L\left\{z\hat{\mathbf{I}}_3\mathbf{C}_{11}\hat{\mathbf{I}}_1^{\mathrm{T}}\left\{\mathbf{H}_5\left(z\right)\right\}_{m\times1}+\tilde{\mathbf{I}}_2\mathbf{C}_{33}\tilde{\mathbf{I}}_1^{\mathrm{T}}\left\{\mathbf{H}_5'\left(z\right)\right\}_{m\times1}-z\hat{\mathbf{I}}_3\mathbf{C}_{12}\left\{\mathbf{H}_5''\left(z\right)\right\}_{m\times1}\right\}dz-\mathbf{C}_{22}\left\{\mathbf{H}_5''\left(0\right)\right\}_{m\times1}$$

$$+\left(\int_0^L z\hat{\mathbf{I}}_3\mathbf{C}_{11}\hat{\mathbf{I}}_2^{\mathrm{T}}dz+\mathbf{C}_{12}^{\mathrm{T}}\hat{\mathbf{I}}_1^{\mathrm{T}}+\mathbf{C}_{12}^{\mathrm{T}}\hat{\mathbf{I}}_2^{\mathrm{T}}\right)\left\{\mathbf{H}_5\left(0\right)\right\}_{m\times1}+\left(\int_0^L z^2\hat{\mathbf{I}}_3\mathbf{C}_{11}\hat{\mathbf{I}}_3^{\mathrm{T}}dz+\int_0^L\tilde{\mathbf{I}}_2\mathbf{C}_{33}\tilde{\mathbf{I}}_2^{\mathrm{T}}dz\right)\left\{\mathbf{H}_5'\left(0\right)\right\}_{m\times1}+$$

$$+\int_0^L z\hat{\mathbf{I}}_3\mathbf{d}_1\left(\mathbf{z}\right)dz-\mathbf{d}_2\left(0\right)+\int_0^L\tilde{\mathbf{I}}_2\mathbf{d}_3\left(\mathbf{z}\right)dz,$$

$$\left\{\mathbf{L}_3\right\}_{m\times1}=\left(-\mathbf{C}_{12}^{\mathrm{T}}\hat{\mathbf{I}}_1^{\mathrm{T}}-\tilde{\mathbf{I}}_1\mathbf{C}_{33}\tilde{\mathbf{I}}_1^{\mathrm{T}}\right)\left\{\mathbf{H}_5'\left(L\right)\right\}_{m\times1}+\mathbf{C}_{22}\left\{\mathbf{H}_5'''\left(L\right)\right\}_{m\times1}+\left(-\mathbf{C}_{12}^{\mathrm{T}}\hat{\mathbf{I}}_3^{\mathrm{T}}-\tilde{\mathbf{I}}_1\mathbf{C}_{33}\tilde{\mathbf{I}}_2^{\mathrm{T}}\right)\left\{\mathbf{H}_5'\left(0\right)\right\}_{m\times1}$$

$$+\mathbf{d}_2'\left(L\right)-\tilde{\mathbf{I}}_1\mathbf{d}_3\left(L\right),$$

$$\left\{\mathbf{L}_4\right\}_{m\times1}=-\mathbf{C}_{12}^{\mathrm{T}}\hat{\mathbf{I}}_1^{\mathrm{T}}\left\{\mathbf{H}_5\left(L\right)\right\}_{m\times1}+\mathbf{C}_{22}\left\{\mathbf{H}_5''\left(L\right)\right\}_{m\times1}-L\mathbf{C}_{12}^{\mathrm{T}}\hat{\mathbf{I}}_3^{\mathrm{T}}\left\{\mathbf{H}_5'\left(0\right)\right\}_{m\times1}-\mathbf{C}_{12}^{\mathrm{T}}\hat{\mathbf{I}}_2^{\mathrm{T}}\left\{\mathbf{H}_5\left(0\right)\right\}_{m\times1}+\mathbf{d}_2\left(L\right),$$

$$\left\{\mathbf{L}_5\right\}_{m\times1}=\int_0^L\left\{\hat{\mathbf{I}}_4\mathbf{C}_{11}\hat{\mathbf{I}}_1^{\mathrm{T}}\left\{\mathbf{H}_5\left(z\right)\right\}-\hat{\mathbf{I}}_4\mathbf{C}_{12}\left\{\mathbf{H}_5''\left(z\right)\right\}+\hat{\mathbf{I}}_4\mathbf{C}_{11}\hat{\mathbf{I}}_2^{\mathrm{T}}\left\{\mathbf{H}_5\left(0\right)\right\}_{m\times1}+\hat{\mathbf{I}}_4\mathbf{C}_{11}\hat{\mathbf{I}}_3^{\mathrm{T}}z\left\{\mathbf{H}_5'\left(0\right)\right\}+\hat{\mathbf{I}}_4\mathbf{d}_1\left(\mathbf{z}\right)\right\}dz,$$

$$\left\{\mathbf{L}_6\right\}_{m\times1}=\int_0^L\left\{z\hat{\mathbf{I}}_5\mathbf{C}_{11}\hat{\mathbf{I}}_1^{\mathrm{T}}\left\{\mathbf{H}_5\left(z\right)\right\}_{m\times1}+\tilde{\mathbf{I}}_3\mathbf{C}_{33}\tilde{\mathbf{I}}_1^{\mathrm{T}}\left\{\mathbf{H}_5'\left(z\right)\right\}_{m\times1}-z\hat{\mathbf{I}}_5\mathbf{C}_{12}\left\{\mathbf{H}_5''\left(z\right)\right\}_{m\times1}+z\hat{\mathbf{I}}_5\mathbf{C}_{11}\hat{\mathbf{I}}_2^{\mathrm{T}}\left\{\mathbf{H}_5\left(0\right)\right\}_{m\times1}+\right.$$

$$\left.+\left(z^2\hat{\mathbf{I}}_5\mathbf{C}_{11}\hat{\mathbf{I}}_3^{\mathrm{T}}+\tilde{\mathbf{I}}_3\mathbf{C}_{33}\tilde{\mathbf{I}}_2^{\mathrm{T}}\right)\left\{\mathbf{H}_5'\left(0\right)\right\}_{m\times1}+z\hat{\mathbf{I}}_5\mathbf{d}_1\left(\mathbf{z}\right)+\tilde{\mathbf{I}}_3\mathbf{d}_3\left(\mathbf{z}\right)\right\}dz,$$

$$\left\{\mathbf{L}_7\right\}_{m\times1}=\int_0^L\left(\hat{\mathbf{I}}_6\mathbf{C}_{11}\hat{\mathbf{I}}_1^{\mathrm{T}}\left\{\mathbf{H}_5\left(z\right)\right\}_{m\times1}-\hat{\mathbf{I}}_6\mathbf{C}_{12}\left\{\mathbf{H}_5''\left(z\right)\right\}_{m\times1}+\hat{\mathbf{I}}_6\mathbf{C}_{11}\hat{\mathbf{I}}_2^{\mathrm{T}}\left\{\mathbf{H}_5\left(0\right)\right\}_{m\times1}+z\hat{\mathbf{I}}_6\mathbf{C}_{11}\hat{\mathbf{I}}_3^{\mathrm{T}}\left\{\mathbf{H}_5'\left(0\right)\right\}_{m\times1}+\hat{\mathbf{I}}_6\mathbf{d}_1\left(\mathbf{z}\right)\right)dz$$

References

Bhimaraddi, A and Chandrashekhara, K (1993), Observations on higher-order beam theory, Journal of Aerospace Engineering, Vol. 6(4), 408-413

Carrera, E., and Guinta, G., (2010), Refined beam theories based on a unified formulation, International journal of applied mechanics, 2(1), 117-143.

547 Challamel N. (2011), Higher-order shear beam theories and enriched continuum, Mechanics Research
548 Communications, 38, 388– 392

549 Chen, D., and Cheng, S., (1983), An analysis of adhesive bonded single-lap joints, Journal of applied mechanics,
550 50(1), 109-115.

551 Corre C., Lebée A., Sab K., Ferradi M. K., and Cespedes, X., (2018) Higher-order beam model with eigenstrains:
552 theory and illustrations, ZAMM Journal of applied mathematics and mechanics: Zeitschrift für angewandte
553 Mathematik und Mechanik, 98:1040–1065.

554 Ding, H., Huang, D., and Wand H, (2005), Analytical solution for fixed-end beam subjected to uniform load, Journal
555 of Zhejiang University SCIENCE, 6A(8), 779-783

556 Erkmen, R.E., and Mohareb, M. (2006a), Nonorthogonal solution for thin-walled members- A finite element
557 formulation, Canadian Journal of Civil Engineering, 33(4), 421-439.

558 Erkmen, R.E., and Mohareb, M. (2006b), Nonorthogonal solution for thin-walled members- applications and
559 modelling considerations, Canadian J. of Civil Engineering, 33(4), 440-450.

560 Erkmen, R. E. and Mohareb, M. (2006c), "Torsion Analysis of Thin-Walled Beams Including Shear Deformation
561 Effects", Thin-walled structures, Vol. 44, pp. 1096-1108

562 Erkmen, R.E., and Mohareb, M. (2008a), Buckling analysis of thin-walled open members – A complementary energy
563 variational principle, Thin Walled Structures, 46(6), 602-617.

564 Erkmen, R.E., and Mohareb, M. (2008b), Buckling analysis of thin-walled open members – A finite element
565 formulation, Thin Walled Structures, 46(6), 602-617.

566 Geng P.S.,. Duan T.C, Li L.X. (2017), An uncoupled higher-order beam theory and its finite element implementation,
567 International Journal of Mechanical Science, 34 (525-531)

568 Groh,R.M., and Weaver, P.M., (2015), Static inconsistencies in certain axiomatic higher-order shear deformation
569 theories for beams, plates and shells, Composite structures, 120, 231-245.

570 Guangyu, S and Voyiadjis, G (2011), A Sixth-Order Theory of Shear Deformable Beams With Variational Consistent
571 Boundary Conditions, Mechanics Research Communications, 38 (388-392)

572 Jha,D.K., Kant,T. and Singh,R.K.,(2013), Stress analysis of transversely loaded functionally graded plates with a
573 higher order shear and normal deformation theory, J. of engineering mechanics, 139(12), 1663-1680.

574 Heyliger, P. R. and Reddy, J. N., (1988), A higher order beam finite element for bending and vibration problems,
575 Journal of Sound and Vibration, 126(2), 309-326.

576 Karama M., Afaq K.S., Mistou S., (2003) Mechanical behaviour of laminated composite beam by the new multi-
577 layered laminated composite structures model with transverse shear stress continuity, Internat. J. Solids Structures
578 40 (6) 1525–1546.

579 Levinson, M., (1981), A new rectangular beam theory, J. Sound and Vibration, 74 (1), 81-87.

580 Mechab, I., Tounsi, A, Benatta, M.A., Adda bedia, E.A. (2008) Deformation of short composite beam using refined
581 theories. J. Math. Anal. Appl., 346 468–479

582 Mucichescu, D.T. (1984), Bounds for stiffness for prismatic beams, Journal of Structural Engineering, 110(6), 1410–
583 1414.

584 Nolde E, Pichugin AV, and Kaplunov J. (2018) An asymptotic higher-order theory for rectangular beams. *Proc. R.*
585 *Soc. A*, **474**: 20180001.

586 Parra, G.J. and Wight J.K. (2002), Prediction of Shear Strength and Shear Distortion in R/C Beam-Column Joints,
587 American Concrete Institute, Michigan, SP197-10.

588 Patel, R., Dubey, S. K., and Pathak, K.K. (2014), Effect of depth span ratio on the behaviour of beams, International
589 Journal of Advanced Structural Engineering, 56(6), 1-7.

590 Pham, P.V. and Mohareb, M. (2014), A shear deformable theory for the analysis of steel beams reinforced with GFRP
591 plates, Thin-Walled Structures, 85, 165-182.

592 Pham, P.V and Mohareb, M. (2015), Nonshear Deformable Theory for Analysis of Steel Beams Reinforced with
593 GFRP Plate Closed-Form Solution, J. Struct. Eng., ASCE, 141(12), 04015063.

594 Pham, P.V, Mohareb, M., and Fam, A., (2018), Finite element formulation for the analysis of multilayered beams
595 based on the principle of stationary complementary strain energy, Engineering Structures, 167, 287-307.

596 Pham, P.V, (2018), Analysis of steel beam strengthened with adhesively-bonded GFRP plates, A PhD thesis,
597 Department of Civil Engineering, University of Ottawa, ON, Canada.

598 Timoshenko, S. P. (1921), On the corrections for shear of the differential equation for transverse vibrations of
599 prismatic bars, Philosophical Magazine, 41, 744-746.

600 Timoshenko, S. P. and Goodier, J., N. (1970), theory of elasticity (McGwaw-Hill, New York).

601 Stephen, N. G. and Levinson, M. (1979), A second order beam theory, Journal of Sound and Vibration, 67 (3), 293-
602 305.

603 Shu, X., and Sun, L., (1994), An improved simply higher order theory for laminated composite plates, Journal of
604 computers and Structures, 50(2), 231-236.

605 Sun, Z., Yang L., Gao, Y., (2015), The displacement boundary conditions for Reddy higher-order shear cantilever
606 beam theory, Acta Mechanica, 226, 1359–1367

607 Reddy, J. (1984), Energy and variational methods in applied mechanics, John Wiley & Sons.

608 Reddy J.N. (2007), Nonlocal theories for bending, buckling and vibration of beams, International Journal of
609 Engineering Science, 45 (2007), 288-307.

610 Zhao, B., Lu, Z.H., and Lu, Y., N., (2014), 2D analytical solution of elastic stresses for balanced single-lap joints-
611 Variational method, Int. J. of Adhesion & Adhesives, 49, 115-126.

612

613

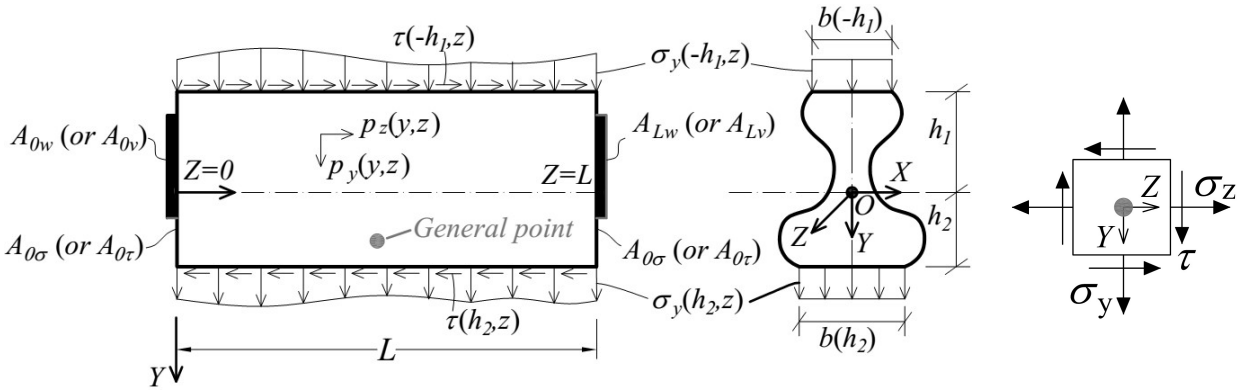

(a) Profile view (b) Cross-section (c) Stress state at a general point

Figure 1 Beam tractions and body forces

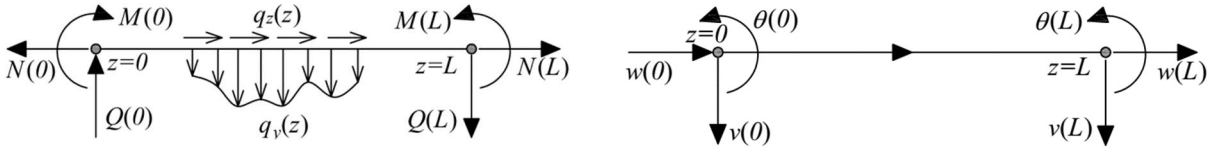

(a) (b)

Figure 2 Sign convention for (a) Resultant line loads and stress resultants and (b) End displacements

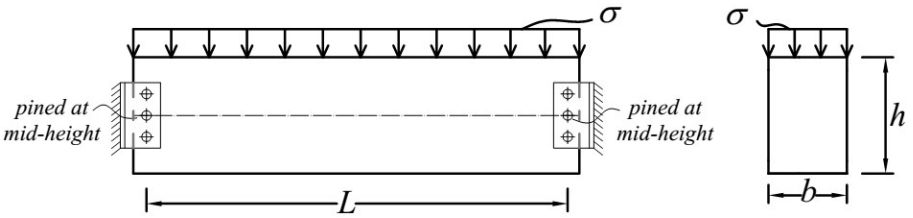

Figure 3 Simply supported beam under a uniform traction

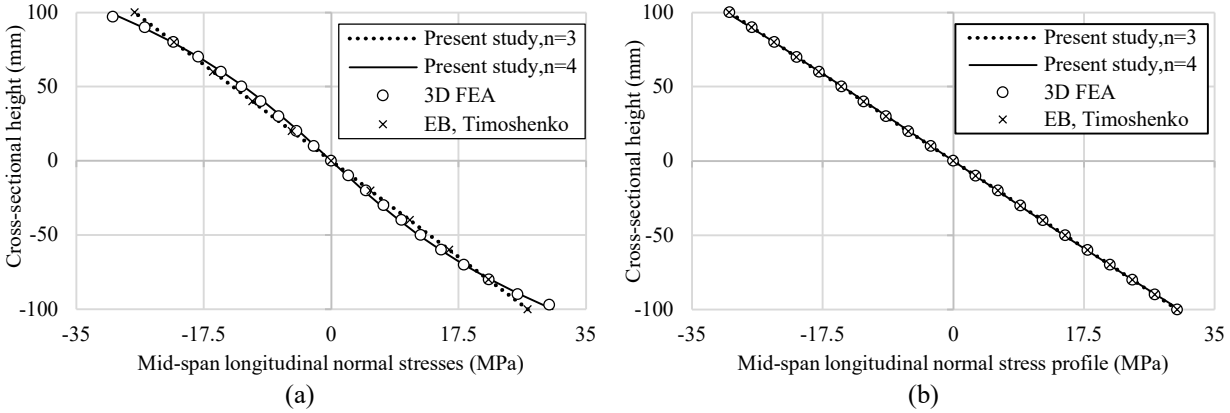

(a) (b)

Figure 4 Longitudinal stress profiles at mid-span cross-section for spans (a) L=3h and (b) L=10h

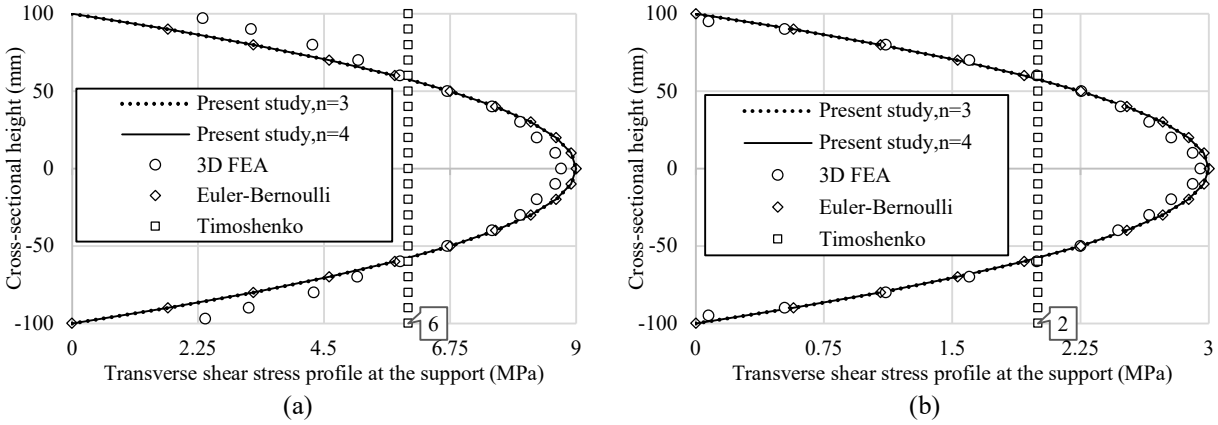

Figure 5 Transverse shear stress profiles at support cross-sections for spans (a) L=3h, (b) L=10h

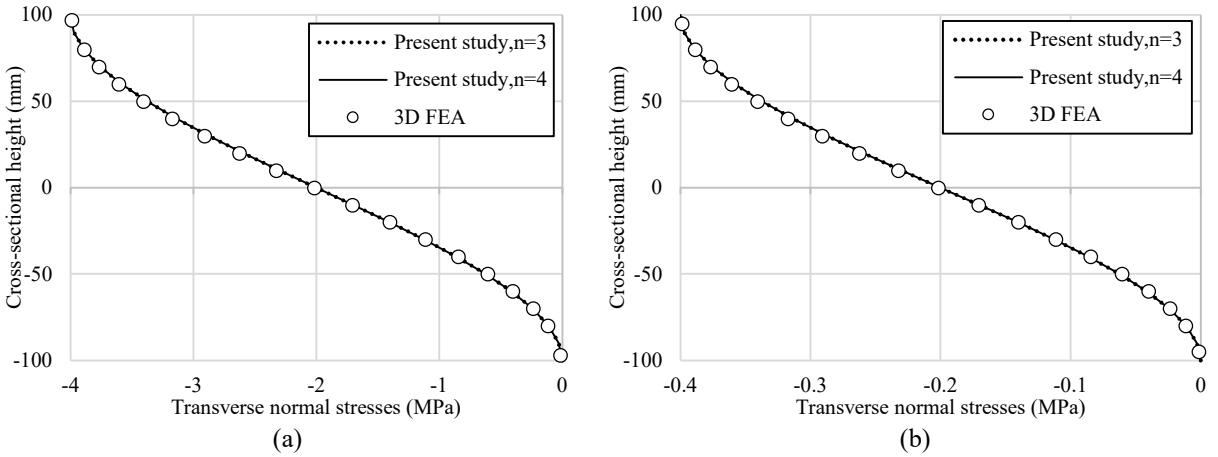

Figure 6 Transverse normal stress profiles at mid-span cross-sections for spans (a) L=3h, (b) L=10h (positive stresses denote tension)

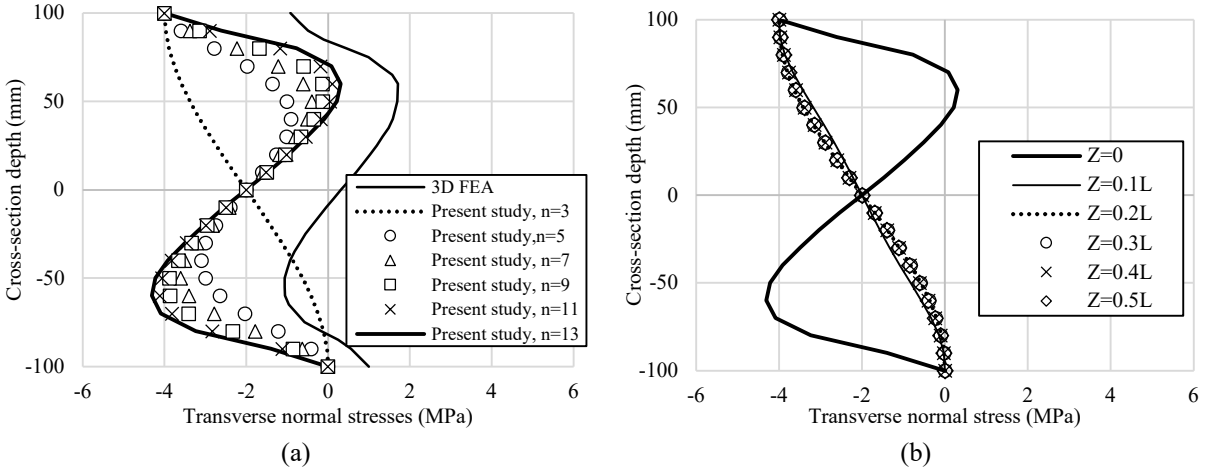

Figure 7 Transverse normal stress profiles for L=3h (a) Effect of the number of terms n (z=0), and (b) Effect of cross-section location Z (n=9)

630

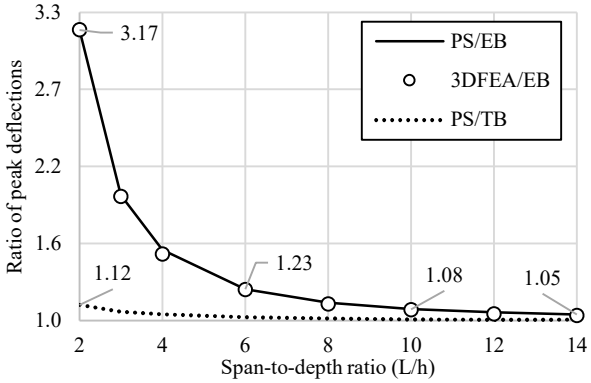

631

632 **Figure 8** Effect of the shear deformation on the prediction of the peak deflection

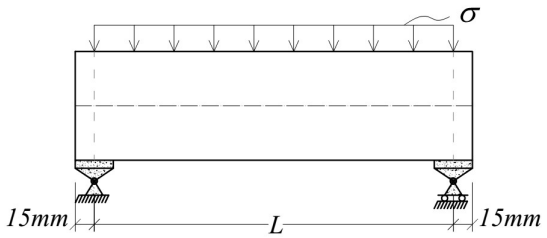

633

634 **Figure 9** Beams simply supported at the bottom fibers

635

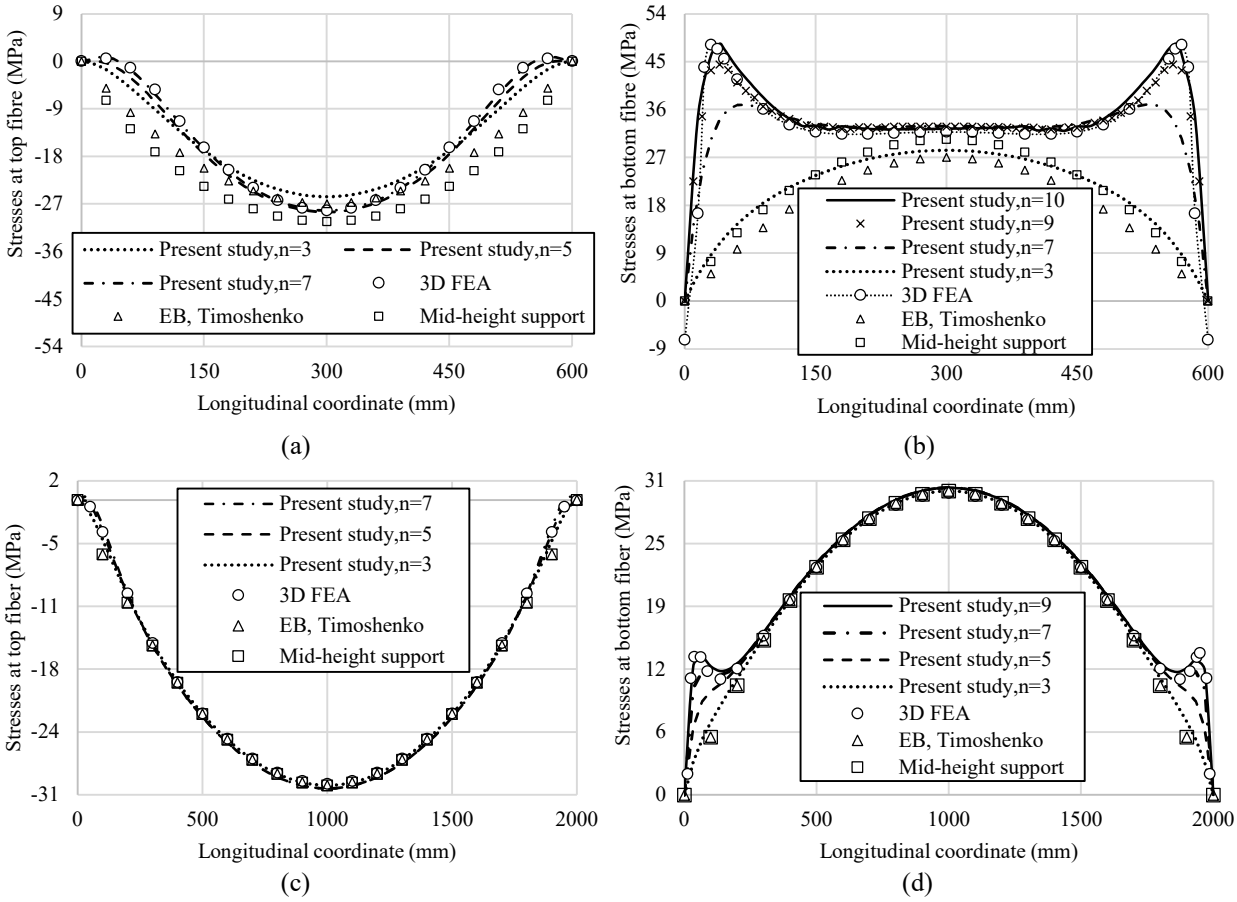

Figure 10 Longitudinal normal stresses for (a) At top fiber L=3h (b) At bottom fiber L-3h, (c) at top fiber L=10h, and b) at bottom fiber L=10h

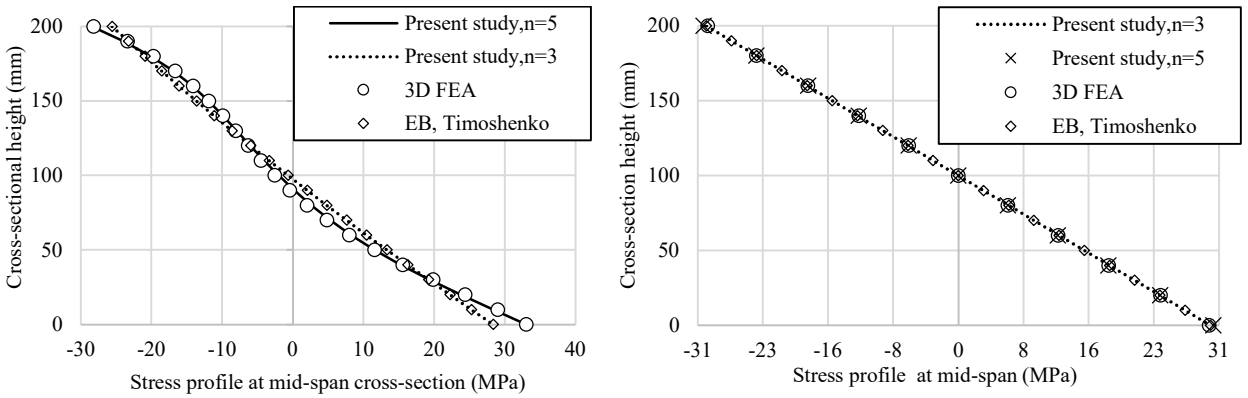

(a) (b)

Figure 11 Longitudinal stress profiles at mid-span cross-section for spans (a) L=3h, (b) L=10h

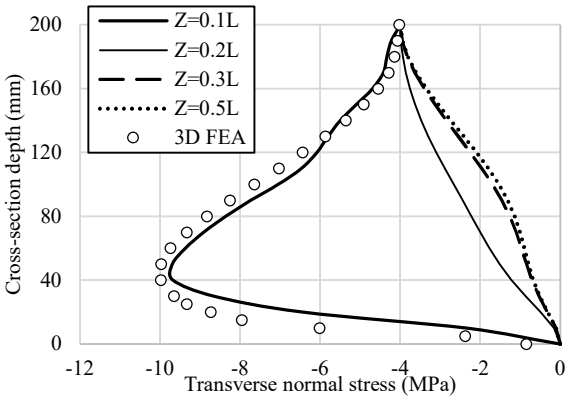

Figure 12 Transverse normal stress profiles at sections z=0.1L, 0.2L, 0.3L, and 0.5L

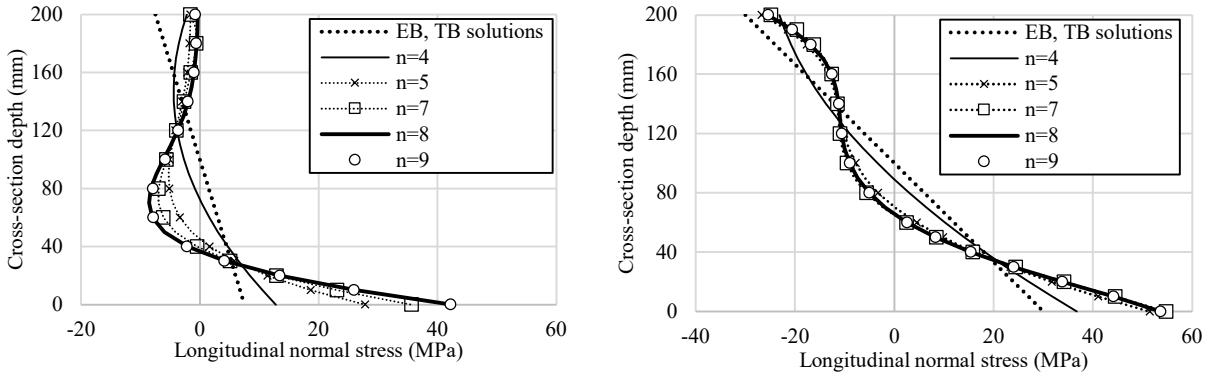

(a) L/h=1 (b) L/h=2

Figure 13 Longitudinal stress profiles at mid-span for spans (a) L=h and (b) L=2h